

Cryopreservation of Dental Stem Cells

Nela Pilbauerová*, Jakub Suchánek

ABSTRACT

Nowadays, regenerative and reparative medicine has grown in popularity. Dental stem cells are easily accessible source of adult stem cells. They can be harvested by a tooth extraction or spontaneous deciduous tooth exfoliation. They have to be isolated, expanded and stored until time they would be needed for individual stem cell therapy. Cryopreservation is both a short-term and long-term storage of tissues or cells at sub-zero temperatures. There are several methods of cryopreservation requiring different technologies. The objective of this review is to compare them and highlight their advantages and disadvantages.

KEYWORDS

cryopreservation; dental stem cells; freezing protocol

AUTHOR AFFILIATIONS

Department of Dentistry, Charles University, Faculty of Medicine in Hradec Králové, and University Hospital, Hradec Králové, Czech Republic

* Corresponding author: Department of Dentistry, University Hospital, Sokolská 581, 500 05 Hradec Králové, Czech Republic; e-mail: nela.pilbauerova@gmail.com

Received: 30 January 2018

Accepted: 16 April 2018

Published online: 2 July 2018

Acta Medica (Hradec Králové) 2018; 61(1): 1–7

<https://doi.org/10.14712/18059694.2018.16>

© 2018 The Authors. This is an open-access article distributed under the terms of the Creative Commons Attribution License (<http://creativecommons.org/licenses/by/4.0>), which permits unrestricted use, distribution, and reproduction in any medium, provided the original author and source are credited.

INTRODUCTION

Stem cells (SCs) have opened promising future in regenerative medicine, because of their two remarkable features known as self-renewal and multilineage differentiation. Based on the SCs origin, they are classified into Embryonic stem cells (ESCs) and Adult (postnatal) stem cells (ASCs). The advantages of ASCs are less ethical concerns, low immunogenicity and less tumorigenic potency than their embryonic counterparts (1). ASCs have been isolated from many human tissues so far, such as dermis (2), peripheral blood (3), adipose tissues (4), intestine (5), cartilage (6) and bone marrow (7). Several types of ASCs have been identified in dental related tissues. ASCs reside in specialized micro-environment called “niche”, which regulates stem cell behavior and maintains a balance between cell death and self-renewal (8).

Dental related tissues represent an easily accessible source of ASCs. Embryologically, human teeth develop from reciprocal interaction between the dental ectoderm (oral epithelium) and the neural crest-derived mesenchyme (dental mesenchyme) (9). Most of the dental tissues have dental mesenchyme origin – dentin, dental pulp, periodontal ligaments, alveolar bone. Enamel is a dental ectoderm derivative. Due to their ectomesenchymal origins, dental stem cells (DSCs) may display characteristics of both mesoderm and ectoderm (10).

Up until now, seven different types of DSCs have been isolated. They are classified in two major groups, dental pulp-related stem cells and periodontium-related stem cells. Dental pulp-related stem cells are: Dental Pulp Stem Cells (DPSCs) (11); Stem cells from Human Exfoliated Deciduous teeth (SHED) (12); and Stem Cells from Apical Papilla (SCAP) (13), and Human Natal Dental Pulp Stem Cells (NDP-SCs) (14). Periodontium-related are: Periodontal Ligament Stem Cells (PDLSCs) (15), Dental Follicle Progenitor Cells (DFPCs) (16), Gingival Mesenchymal Stem Cells (GMSCs) (17). DPSCs were first identified by Gronthos et al. in 2000. And 3 years later, in 2003, Miura et al. first isolated SHED.

As it has been already mentioned, DSCs are easily accessible by a tooth extraction among younger individuals or when a primary tooth is exfoliated. However, these tooth extractions or spontaneous exfoliations usually occur in a period of life when there is normally no need for a stem cell therapy. Therefore, it is necessary to isolate, expand and store stem cells until the time when they would be required.

PRINCIPLES OF CRYOPRESERVATION

Cryopreservation is a process of sustaining the viability of cells and tissues by freezing and storing them at sub-zero temperatures, when biochemical reactions do not occur (18). DSCs can be subject to an irreversible damage during the freezing or thawing process, known as a freezing injury (19). An exact mechanism is poorly understood, but in general, the irreversible changes to the DSCs are explained by extracellular and intracellular forming of ice crystals. There are two key mechanisms. The first one occurs, when DSCs are cooled slowly, and the extracellular ice crystal

formation causes an osmotic efflux of water from cells. This mechanism increases the concentration of intracellular solutes, which can lead to an osmotic damage because of the solute toxicity. The other one happens, when DSCs are cooled rapidly. Because of that, there is not enough time for water to leave the cells and the intracellular formation of ice crystals causes mechanical and structural damages to the cells (20).

Other freezing-associated stress is a creation of reactive oxygen species (ROS), which are possible triggers for apoptosis (21).

To avoid that, there is a cryoprotective agent (CPA) incorporated into the freezing medium to protect DSCs during both the freezing and thawing process. The major effects of CPAs are to optimize the cooling rate and to block the formation of ice crystals by binding to nuclei and slowing down ice crystals growing (22).

CRYOPRESERVATION OF WHOLE TEETH

Although the main area of interest of short or long-term cryopreservation studies of DSCs is the cryostorage of dental stem cell lineages after their successful isolation and expansion from the dental related tissues, there have been several attempts to cryopreserve whole, both deciduous and permanent, intact teeth. Dental stem cell isolation and expansion in a lab environment is expensive, time consuming and risky for contamination and spontaneous differentiation (23). The hypothesis, why to bank intact whole teeth, was to postpone these procedures till later time, when DSCs would be actually required. However, many limitations remain in this method as well, which make its clinical use practically impossible. One of the problems is the low percentage of viable DSCs obtained from cryopreserved deciduous or permanent teeth after the thawing process. Liedemann et al. showed in their study that DPSCs were obtained from cryopreserved deciduous teeth only with a 30% culture rate, whereas from non-cryopreserved teeth, this rate increases to 61% (23). In another research, Woods et al. used permanent immature teeth with not fully developed roots and they observed only a 20% isolation rate after thawing. For them, 3 out of 10 cryopreserved teeth did not contain any stem cells showing morphological characteristics of DPSCs or they exhibited no cell growth whatsoever. Plus, in post-thawing observations the cryopreserved DPSCs had a low proliferation rate and round-shaped cytoplasm, compared with spindle-shaped cytoplasm of non-cryopreserved group (23). The low isolation rate might be associated with low penetration and diffusion of the CPA into the center of the dental pulp and therefore the insufficient protection from the ice crystal formation. Because of that, deciduous teeth with no visible root resorption or permanent teeth with fully developed roots cannot be used. On the other hand, root resorption or open root apices provide a way of penetration for the CPA. Yet the proliferation rate remains very low, in particular to meet the clinical demands. There was also an attempt to modify the freezing protocol by using Nd:YAG laser piercing, which makes micro-holes into the tooth surface and facilitate penetration of CPA (25). The

isolation rate of DPSCs during this novel method was similar to the rate of non-cryopreserved DPSCs. However, the costs and difficulty were significantly higher. The other causes of DPSC damage may be due to the tooth fractures that might occur after low temperature exposure during freezing process. For now, this method does not show repeatable and satisfiable results in DPSC cryopreservation and it does not allow its application in therapeutic purposes.

INTERNATIONAL LICENSED DENTAL STEM CELL BANKS

According to recently published studies, the cryopreservation of isolated lineages of DSCs remains the method with the most successful cryorecovery results. This conclusion is very important in answering the question if cell banks should bank whole intact teeth or the isolated stem cell populations. Another hypothesis can also be that a minimal manipulation with the pulpal tissues before the freezing might yield better results of post-thawed viable DPSCs. Wood et al. disproved this idea; DPSCs digested from post-thaw pulp tissue did not proliferate at the same rate observed in their fresh counterparts. It took at least twice as long (24).

Current number of licensed dental stem cell banks is very low. Historically the first one was built in Japan at Hiroshima University in 2005 (26). The National tooth bank was opened soon after in 2008. Another was open in Norway thanks to the collaboration between Norwegian Institute of Public Health and the University of Bergen (27). There are also commercially licensed tooth banks in the UK and the USA.

CRYOPRESERVATION PROCEDURE OF ISOLATED POPULATION OF DSCS

When DSCs are intended to use for therapeutic purposes the entire cryopreservation thawing protocol must follow standards of good manufacturing practice (cGMP).

TOOTH COLLECTION

In general, each vital tooth both deciduous and permanent might be a potential source of dental related stem cells. However, one of the major problems associated with cryopreservation is that the degrading process of dental related tissues starts immediately after the tooth is extracted or exfoliated. Several previous studies established the maximum time frame for stem cell isolation to be 120 hours post extraction (24, 28). The longer time frame from the tooth extraction, the lower post thawing cell recovery efficiency is observed (28). A submersion of the tooth into a sterile hypotonic phosphate-buffered saline solution while the tooth is transported to a laboratory for DSC harvesting and isolation prevents dental tissue necrosis to begin. This solution precludes tooth dehydration. Transported teeth

have to be kept in hypothermic conditions (at 4 °C), which is being referred to as a sustention.

A tooth extraction, as a future source of DPSCs, is a common surgical procedure, which can be performed at any age. Dental pulp tissues from wisdom teeth are the most common source of DPSCs among adults. The second most common are premolars. In particular, first premolars are often extracted during an orthodontic treatment of frontal teeth crowding. In general, the efficiency of DPSC harvesting and isolation is higher when the permanent teeth are immature and they do not have fully developed roots. In deciduous teeth, as sources of SHED, vital pulp tissues are mainly found in clinical crowns. Their roots must not be resorbed more than 1/3 of the original length. The greater root resorption might have a negative impact on the viability of SHED (29).

Harvested teeth should be washed out in commercially available bactericidal solutions, e. g. chlorhexidine, to minimize the bacterial contamination. It helps to further reduce the risk of cross-contamination (24).

DENTAL PULP STEM CELL ISOLATION AND EXPANSION

As soon as a tooth is collected and transported to the laboratory, the dental crown is gently separated from the root to open the pulp chamber and harvest the pulp tissue. There are several methods how to perform that allowing for a minimal damage to the cellular components. First, undeveloped roots in permanent teeth or resorbed roots in deciduous teeth have largely open apices (usually more than 2 mm). These open roots create a way to obtain pulp tissues through them without a necessity of splitting the crown from the root. The other approach, if the apical foramina are too narrow, is to use special forceps or diamond burs and gently open the pulp chamber in the cervical third of the tooth, at the enamel - cementum junction. Indeed, the possibility of an irreversible damage to pulp tissues is higher with this method. Afterwards, the dental pulp is gently separated from the pulp chamber and root canal walls and minced into small pieces.

In order to isolate DPSCs there are also two approaches. DPSCs can be isolated either by an enzymatic digestion (ED) method (30, 31) or a spontaneous outgrowth (OG) method (32, 33).

To perform the first method, pulp tissue fragments are digested by submerging them into a solution of enzymes collagenase type I and dispase, or trypsin enzyme to obtain single cell suspension. The second approach, on the other hand, is based on a spontaneous stem cell overgrowth from minced pulp tissue pieces. Several researchers have tried to answer a question which method has better efficiency of cell proliferation rate or unchanged morphological and phenotypic properties of isolated stem cells. Unfortunately, while some researchers concluded that stem cells isolated by OG have lower proliferation rate and weaker stem cells marker expression (34), some others concluded no differences in those aspects regardless of the isolation method used (35). Thus more detailed studies are further required to answer this question.

CRYOPRESERVATION SOLUTION

The high-water content of tissues and cells is one of the leading determinants of physical changes during the freezing or thawing phase of cryopreservation. During sub-zero temperatures formation of ice crystals occurs, which can lead to a fatal damage to tissues and cells.

A cryoprotective agent (CPA) is incorporated into the cryopreservation medium in order to protect stem cells from the ice crystal formation. Major attribute of CPAs is determined by their ability to reduce the freezing and thawing point and therefore optimize the freezing rate (22). Currently used CPAs are divided into two major groups. First one are low molecular weight substances, for example glycerol, ethylene (propylene) glycol, dimethyl sulfoxide (DMSO), which can penetrate a cell cytoplasmic membrane, prevent the formation of ice crystal nuclei and slow down the ice crystal growth inside cells (36). Contrary, the second group includes substances with high molecular weight, for example, dextran, hydroxyethyl starch (HES), polyvinylpyrrolidone and polyvinyl alcohol. They remain in the extracellular space and allow for cell dehydration and minimization of the intracellular ice crystal formation, and stabilize the cellular membrane (22).

A freezing medium containing DMSO as the CPA has been widely used in both in vitro and in vivo, since its high efficiency in cell protection was documented. The review of recent literature has shown 10% concentration of the DMSO as the most effective. However, there are some documented concerns about its cytotoxicity and related side effects such as sickness if it is introduced to patients as part of the stem cell therapy (36).

Interestingly, even the knowledge of these side effects has not stopped the usage of DMSO as the CPA, because there is not such as effective alternative. The theory, how to decrease DMSO concentration and the cytotoxic effect as well, is its combination with substances with the high molecular weight. In some recent studies the combination of DMSO and HES has been documented as an effectual alternative in stem cell cryopreservation (22, 37).

Another question is the optimal cell concentration for cryopreservation to maximize the post-thaw cell viability. Woods et al. at indicated that $1.0 - 1.5 \times 10^6$ cell (with 10% DMSO as the CPA) yielded optimal results (24).

Furthermore, a xenogeneic serum is the most commonly incorporated into the standard used freezing medium. However, the presence of the fetal calf serum/bovine serum is against standards of cGMP, in particular in the human stem cell therapy. Therefore, one of the major interests of further researchers should be to comprehensively examine the efficiency of the serum-free freezing medium that contains the non-toxic CPA in DSC cryopreservation.

FREEZING PROTOCOL

There are several techniques of the freezing protocol. However, a choice among those methods depends on resources available and experience of scientists and technicians.

CONTROLLED-RATE FREEZING

The goal of minimizing the potential for stem cell damage by dehydration and ice crystal formation during cryopreservation led to the introduction of controlled-rate freezing methods. The slow freezing rate (SRF), 1–2 °C per minute, is generally considered as optimal for maintaining stem cell viability during cryopreservation (38, 39). Other method, ultra-slow freezing rate (USFR), is the highly controlled rate of 0.3 to 0.6 °C per minute, which is more costly (40). Current studies have shown significantly higher post-thaw cell growth and viability using those methods, in contrast with the rapid freezing method described below. For instance, Huynh et al. concluded that controlled-rate freezing methods resulted in a significantly higher number of viable cells, both in 5% and 10% DMSO (79.7% and 79.0% respectively) compared with the rapid freezing method (41). At the same time, Naaldijk et al. observed the effect of different freezing rates during cryopreservation of rat mesenchymal stem cells and they determined, on the other hand, that the rapid freezing protocol is no less effective in maintaining post-thaw viability of MSC compared to the controlled rate freezing method. They also showed, that different effect of freezing protocols are only observable 3 days after thawing and beyond (37).

In addition, another problematic issue is that these methods cannot be scaled up to provide uniformity of temperature to all vials during large scale banking. Thus, further development in this area is necessary (42).

UNCONTROLLED-RATE FREEZING

The alternative approach of cryopreservation is an uncontrolled rate freezing protocol. The CPA and tissue or stem cell samples are first precooled to 4 °C and then they are directly deposited into the freezer at –80 °C or into liquid nitrogen (43). This process is considered to be a simpler, cheaper alternative that requires no individual training or specific technology. Current research has determined uncontrolled rate freezing to be an efficient method in long-term cryopreservation of DPSCs (44). It also concluded no post-thaw effect on cell viability, multipotency, proliferation and differentiation. However, the efficiency of uncontrolled rate freezing protocol has so far only been studied in the presence of 10% DMSO as the CPA.

RAPID FREEZING (VITRIFICATION)

The principle of the rapid freezing protocol is based on the formation of an arrested liquid state and a glasslike solidification in presence of a high concentration of the CPA (45). This method has been well described in the cryopreservation of human embryonic stem cells, oocytes, sperms, which are particularly sensitive to cryoinjuries. For instance, Jadoon et al. concluded that the greater amount of vitrified oocytes survived cryopreservation through rapid freezing than slowly frozen (SRF) oocytes (70.3% vs. 12.5%) in their study in 2015 (46). On the other site, there are very

few published papers concerning the usage of the rapid freezing method in cryopreservation of DSCs. Huynh et al. compared the post-thaw cell viability and the growth rate of DPSCs cryopreserved by controlled-rate freezing and rapid freezing method in 5% and 10% DMSO. Regardless the percentage of DMSO used, DPSCs cryopreserved for 6 months by the latter method did not regrow after thawing. In comparison to it, the former method resulted in significant higher number of viable cells and the more rapid growth rate (47). Unfortunately, this approach also seems to be unsuccessful in cryopreservation of whole intact teeth, due to progressive root resorption and the damage of DSCs embedded in the hard dental tissues (48). The concept of this technique is to isolate small volume of the tissue specimen, which is going to be cryopreserved, and to place them on vitrification carriers, such as cryoleaf, cryoloop, or ministraw, directly into a liquid nitrogen (49, 50). It is a very simple technique. Interestingly the possible toxic effect of the DMSO as the CPA can be minimized by rapid freezing rate (51). Unfortunately, just the small volume of samples and relatively high volume of liquid nitrogen for each vitrification, carries limit this technology to scale up for wider clinical use.

MAGNETIC FREEZING

Magnetic cryopreservation is considered to be a controlled slow-rate freezing technique. Programed freezers are supplied with a magnetic field of 0.01 mT and they cool at the rate of 0.5 °C/min until the temperature reaches -32 °C (52). Afterwards, the cryopreserved samples are stored in a -150 °C freezer. The magnetic field has been proven to lower water aggregation during freezing. This is advantageous as formation of ice crystals as well as a generation of unwanted weak electric current are both reduced. Therefore, the electric current cannot disrupt cell membranes, which allows for a better protection of cells during freezing (53). It has been published so far that this technique can be effective in the cryopreservation of both, whole intact teeth as well as isolated DPSCs. Lee SY, Sun CH, Kuo TF et al. observed the effect of the magnetic cryopreservation on intact rat teeth and pulpal tissues in the presence of different concentration of the DMSO as the CPA. Still, they observed a problematic penetration of the CPA into the coronal part of the pulp tissue while cryopreserving intact teeth, however, a better penetration to the root portion of the teeth has been seen. At the end, they concluded that the magnetic cryopreservation is still an effective method for intact tooth and pulp tissue banking compared to the others. It requires lower concentration of DMSO and shorter pre-equilibration time. Finally, it allows higher biological activity of the recovered DPSCs from post-thawed tooth and pulp tissue (53). DPSCs isolated from the magnetic cryopreservation contained 73% of viable cells (54). Additionally, this method also revealed successful results for cryopreservation of DPSCs in presence of 3% DMSO and a serum-free cryopreservation medium (SFM). This seems very promising for good manufacturing practice (cGMP) and therefore for further application in human regenerative medicine (52).

OPTIMAL STORAGE TEMPERATURE

The viability of post-thawed DPSCs, stored for 1 week, 1 month or 6 months at either -85 °C or -196 °C, was $\geq 90\%$ for all storage lengths and both temperatures. No variations in the doubling time or in the differential potential were significant statistically (24).

CELL THAWING

There have been very few research papers concerning the optimal thawing method or the thawing temperature. The most widespread standard procedure, that has been utilized so far, is a 37 °C water bath. It has been proven that this technique removes ice crystals efficiently and the potential cell damage is minimal (28, 55). On the other hand, water environment brings a high risk for bacterial or fungicidal contamination. Other method, that has been studied up to now, is the application of dry heat. These studies identified that samples thawed using dry heat had similar viabilities and clonogenic potential to those thawed using the standard water procedure (56, 57). The different thawing temperature (0, 20 and 37 °C for 20 min) did not uncover any statistically significant changes on post-thawed cells (58). However, this is only a one study and this area ought to be examined more comprehensively before a generally valid conclusion can be drawn.

In any case, The CPA should be washed out from cryovials after thawing due to its cytotoxic effect, DMSO in particular. This approach has been standardized in thawing of cells of bone marrow and peripheral blood. The problematic step of the CPA removal is that cells first shrink and then swell, which may cause their damage as well. Because of it a stepwise removal of the CPA, using graded isotonic solutions, is recommended. However, recently published studies concerning cryopreservation and thawing of DPSCs incorporated either the stepwise removal of the CPA or no rinsing steps at all.

CONCLUSION

Over the recent years, reparative and regenerative medicine has been grown in popularity. DSCs represent a relatively simple to obtain sources of adult stem cells with minimal harm to the donor individuals. Both, cryopreserved intact tooth or DSCs, can be further use in individual regenerative cell and tissue therapy. As such, the most optimized cryopreservation protocol for both has to be established. However, the question what optimal is remains to be addressed. What is the optimal concentration of the CPA? Is there any non-toxic CPA or serum-free freezing medium, which has no cytotoxic effect and yields efficient results for the post-thaw cell viability? What is the optimal cryopreservation method with successful results, but is not overly costly and does not require specific technology? Among other questions there is an area of the long-term cryopreservation (>10 years) and its negative effects on cryopreserved tissues and cells. It is clear, that an optimal cryopreservation protocol remains to be a relatively un-

explored field with lots of questions and less answers and further comprehensive research is required before valid conclusions can be drawn.

REFERENCES

- Potdar PD, Jethmalani YD. Human dental pulp stem cells: applications in future regenerative medicine. *World J Stem Cells* 2015; 7(5): 839-51.
- Toma JG, Akhavan M, Fernandes KJ et al. Isolation of multipotent adult stem cells from the dermis of mammalian skin. *Nat Cell Biol* 2001; 3(9): 778-84.
- Zvaifler NJ, Marinova-Mutafchieva L, Adams G et al. Mesenchymal precursor cells in the blood of normal individuals. *Arthritis Res* 2000; 2(6): 477-88.
- Zuk PA, Zhu M, Ashjian P et al. Human adipose tissue is a source of multipotent stem cells. *Mol Biol Cell* 2002; 13(12): 4279-95.
- Wong MH. Regulation of intestinal stem cells. *J Invest Dermatol Symp Proc* 2004; 9: 224-8.
- Alsalameh S, Amin R, Gemba T et al. Identification of mesenchymal progenitor cells in normal and osteoarthritic human articular cartilage. *Arthritis Rheum* 2004; 50(5): 1522-32.
- Friedenstein AJ, Chailakhjan RK, Lalykina KS. The development of fibroblast colonies in monolayer cultures of guinea-pig bone marrow and spleen cells. *Cell Tissue Kinet* 1970; 3(4): 393-403.
- Morrison SJ, Spradling AC. Stem cells and niches: mechanisms that promote stem cell maintenance throughout life. *Cell* 2008; 132(4): 598-611.
- Miletich I, Sharpe PT. Neural crest contribution to mammalian tooth formation. *Birth Defects Res C Embryo Today* 2004; 72(2): 200-12.
- Huang GT, Gronthos S, Shi S. Mesenchymal stem cells derived from dental tissues vs. those from other sources: their biology and role in regenerative medicine. *J Dent Res* 2009; 88(9): 792-806.
- Gronthos S, Mankani M, Brahimi J et al. Postnatal human dental pulp stem cells (DPSCs) in vitro and in vivo. *Proc Natl Acad Sci USA* 2000; 97(25): 13625-30.
- Miura M, Gronthos S, Zhao M et al. SHED: stem cells from human exfoliated deciduous teeth. *Proc Natl Acad Sci USA* 2003; 100: 5807-12.
- Sonoyama W, Liu Y, Fang D et al. Mesenchymal stem cell-mediated functional tooth regeneration in swine. *PLoS One* 2006; 1: 79.
- Karaöz E, Doğan BN, Aksoy A et al. Isolation and in vitro characterization of dental pulp stem cells from natal teeth. *Histochem Cell Biol* 2010; 133(1): 95-112.
- Seo BM, Miura M, Gronthos S et al. Investigation of multipotent postnatal stem cells from human periodontal ligament. *Lancet* 2004; 364(9429): 149-55.
- Morsczeck C, Götz W, Schierholz J et al. Isolation of precursor cells (PCs) from human dental follicle of wisdom teeth. *Matrix Biol* 2005; 24(2): 155-65.
- Zhang Q, Shi S, Liu Y et al. Mesenchymal stem cells derived from human gingiva are capable of immunomodulatory functions and ameliorate inflammation-related tissue destruction in experimental colitis. *J Immunol* 2009; 183(12): 7787-98.
- Mullen F, Critser JK. The science of cryobiology. *Cancer Treat Res* 2007; 138: 83-109.
- Zhurava M, Woods EJ, Acker JP. Intracellular ice formation in confluent monolayers of human dental stem cells and membrane damage. *Cryobiology* 2001; 61: 133-41.
- Mazur P, Leibo SP, Chu EH. A two-factor hypothesis of freezing injury. Evidence from Chinese hamster tissue-culture cells. *Exp. Cell Res* 1972; 71(2): 345-55.
- Mazzilli F, Rossi T, Sabatini L et al. Human sperm cryopreservation and reactive oxygen species (ROS) production. *Acta Eur Fert* 1995; 26(4): 145-8.
- Stolzinger A, Naaldijk Y, Fedorova V, Sethe S. Hydroxyethylstarch in cryopreservation - Mechanisms, benefits and problems - review. *Transfusion and Apheresis Science* 2012; 46: 137-47.
- Lindemann D, Werle SB, Steffens D. Effects of Cryopreservation on the characteristics of Dental Pulp Stem Cells of Intact Deciduous teeth. *Archives of oral biology* 2014; 59: 970-76.
- Woods J, Perry BC, Hockema JJ et al. Optimized Cryopreservation Method for Human Dental Pulp-Derived Stem Cells and Their Tissues of Origin for Banking and Clinical Use. *Cryobiology* 2009; 59(2): 150-7.
- Gioventiu S, Andriolo G, Bonino F et al. A Novel Method for Banking Dental Pulp Stem Cells. *Transfusion and Apheresis Science* 2012; 47: 199-206.
- Abedini S, Kaku M, Kawata T et al. Effects of cryopreservation with a newly-developed magnetic field programmed freezer on periodontal ligament cells and pulp tissues. *Cryobiology* 2001; 62(3): 181-7.
- Tvinnereim HM, Lygre GB, Haug K et al. A biobank of primary teeth within the Norwegian mother and child cohort study (MoBa) per 2014: a resource for the future. *Norsk Epidemiologi* 2014; 24(1-2): 135-40.
- Perry BC, Zhou D, Wu X, et al. Collection, cryopreservation, and characterization of human dental pulp-derived mesenchymal stem cells for banking and clinical use. *Tissue Eng C Methods* 2008; 14(2): 149-56.
- Bernardi L, Luisi SB, Fernandes R et al. The isolation of stem cells from human deciduous teeth pulp is related to the physiological process of resorption. *J Endod* 2011; 37(7): 973-9.
- Gronthos S, Mankani M, Brahimi J et al. Postnatal human dental pulp stem cells (DPSCs) in vitro and in vivo. *Proc Natl Acad Sci USA* 2000; 97(25): 13625-30.
- Suchanek J, Soukup T, Ivanakova R et al. Human dental pulp stem cells-isolation and long term cultivation. *Acta Medica* 2007; 50(3): 195-201.
- Park SH, Hsiao GY, Huang GT. Role of substance P and calcitonin gene-related peptide in the regulation of interleukin-8 and monocyte chemoattractant protein-1 expression in human dental pulp. *Int Endod J* 2004; 37(3): 185-92.
- Spath L, Rotilio V, Alessandrini M et al. Explant-derived human dental pulp stem cells enhance differentiation and proliferation potentials. *J Cell Mol Med* 2010; 14(6B): 1635-44.
- Karamzadeh R, Eslaminejad MB, Aflatoonian R. Isolation, characterization and comparative differentiation of human dental pulp stem cells derived from permanent teeth by using two different methods. *J Vis Exp* 2012; 69: 4372.
- Hilkens P, Gervois P, Fanton Y et al. Effect of isolation methodology on stem cell properties and multilineage differentiation potential of human dental pulp stem cells. *Cell Tissue Res* 2013; 353(1): 65-78.
- Zambelli A, Poggi D, Da Prada G et al. Clinical toxicity of cryopreserved circulating progenitor cells infusion. *Anticancer Res* 1998; 18(6B): 4705-8.
- Naaldijk Y, Staude M, Fedorova V et al. Effect of different freezing rates during cryopreservation of rat mesenchymal stem cells using combinations of hydroxyethyl starch and dimethylsulfoxide. *BMC Biotechnol* 2012; 12: 49.
- Kawasaki N, Hamamoto Y, Nakajima T et al. Periodontal regeneration of transplanted rat molars after cryopreservation. *Arch Oral Biol* 2004; 49(1): 59-69.
- Thirumala S, Zvonic S, Floyd E et al. Effect of various freezing parameters on the immediate post-thaw membrane integrity of adipose tissue derived adult stem cells. *Biotechnol Prog* 2005; 21(5): 1511-24.
- Ha SY, Jee BC, Suh CS et al. Cryopreservation of human embryonic stem cells without the use of a programmable freezer. *Hum Reprod* 2005; 20(7): 1779-85.
- Huynh NC-N, Le SH, Doan VN, Ngo LTQ, Tran HLB. Simplified conditions for storing and cryopreservation of dental pulp stem cells. *Archives of Oral Biology* 2013; 84: 74-81.
- Thirumala S, Goebel WS, Woods EJ. Manufacturing and banking of mesenchymal stem cells. *Expert Opin Biol Ther* 2013; 13: 673-91.
- Davies OG, Smith AJ, Cooper PR et al. The effects of cryopreservation on cells isolated from adipose, bone marrow and dental pulp tissues. *Cryobiology* 2014; 69(2): 342-7.
- Kumar A, Bhattacharyya S, Rattan V. Effect of uncontrolled freezing on biological characteristics of human dental pulp stem cells. *Cell Tissue Bank* 2015; 16(4): 513-22.
- Li T, Mai Q, Gao J et al. Cryopreservation of human embryonic stem cells with a new bulk vitrification method. *Biol Reprod* 2010; 82(5): 848-53.
- Jadoon S, Adeel M. Cryopreservation of oocytes. *J Ayub Med Coll Abbottabad* 2015; 27(1): 22-8.
- Huynh NC, Le SH, Doan VN, Ngo LTQ, Tran HLB. Simplified conditions for storing and cryopreservation of dental pulp stem cells. *Arch Oral Biol*. 2017 Dec; 84: 74-81.
- Kawasaki N, Hamamoto Y, Nakajima T et al. Periodontal regeneration of transplanted rat molars after cryopreservation. *Arch Oral Biol* 2004; 49(1): 59-69.
- Chian RC, Gilbert L, Huang JY et al. Live birth after vitrification of in vitro matured human oocytes. *Fertil Steril* 2009; 91: 372-6.
- Liebermann J, Tucker MJ. Effect of carrier system on the yield of human oocytes and embryos as assessed by survival and developmental potential after vitrification. *Reproduction* 2002; 124: 483-9.
- Kuleshova LL, Lopata A. Vitrification can be more favourable than slow cooling. *Fertil Steril* 2002; 78(3): 449-54.
- Lee SY, Huang GW, Shiung JN et al. Magnetic cryopreservation for dental pulp stem cells. *Cells Tissues Organs* 2002; 196: 23-33.

53. Lee SY, Sun CH, Kuo TF et al. Determination of cryoprotectant for magnetic cryopreservation of dental pulp tissue. *Tissue Eng Part C Methods* 2012; 18(6): 397–440.
54. Lee SY, Chiang PC, Tsai YH et al. Effects of cryopreservation of intact teeth on the isolated dental pulp stem cells. *J Endod* 2010; 36(8): 1336–40.
55. Katayama Y, Yano T, Bessho A et al. The effects of a simplified method for cryopreservation and thawing procedures on peripheral blood stem cells. *Bone Marrow Transplant* 1997; 19(3): 283–7.
56. Röllig C, Babatz J, Wagner I et al. Thawing of cryopreserved mobilized peripheral blood—comparison between waterbath and dry warming device. *Cytotherapy* 2002; 4(6): 551–5.
57. Triana E, Ortega S, Azgueta C et al. Thawing of cryopreserved hematopoietic progenitor cells from apheresis with a new dry-warming device. *Transfusion* 2013; 53(1): 85–90.
58. Yang H, Acker JP, Hannon J et al. Damage and protection of UC blood cells during cryopreservation. *Cytotherapy* 2001; 3(5): 377–386.

Exhaled Breath Condensate: Pilot Study of the Method and Initial Experience in Healthy Subjects

Eva Peterová^{1,2,*}, Jaroslav Chládek³, Darina Kohoutová¹, Veronika Knoblochová¹, Paula Morávková¹, Jaroslava Vávrová⁴, Martina Řezáčová², Jan Bureš¹

ABSTRACT

Analysis of Exhaled breath condensate (EBC) is a re-discovered approach to monitoring the course of the disease and reduce invasive methods of patient investigation. However, the major disadvantage and shortcoming of the EBC is lack of reliable and reproducible standardization of the method. Despite many articles published on EBC, until now there is no clear consensus on whether the analysis of EBC can provide a clue to diagnosis of the diseases. The purpose of this paper is to investigate our own method, to search for possible standardization and to obtain our own initial experience. Thirty healthy volunteers provided the EBC, in which we monitored the density, pH, protein, chloride and urea concentration. Our results show that EBC pH is influenced by smoking, and urea concentrations are affected by the gender of subjects. Age of subjects does not play a role. The smallest coefficient of variation between individual volunteers is for density determination. Current limitations of EBC measurements are the low concentration of many biomarkers. Standardization needs to be specific for each individual biomarker, with focusing on optimal condensate collection. EBC analysis has a potential become diagnostic test, not only for lung diseases.

KEYWORDS

exhaled breath condensate; standardization; healthy subjects

AUTHOR AFFILIATIONS

¹ 2nd Department of Internal Medicine – Gastroenterology, Charles University, Faculty of Medicine in Hradec Králové, University Hospital Hradec Králové, Czech Republic

² Department of Medical Biochemistry, Charles University, Faculty of Medicine in Hradec Králové, Czech Republic

³ Department of Pharmacology, Charles University, Faculty of Medicine in Hradec Králové, Czech Republic

⁴ Institute of Clinical Biochemistry and Diagnostics, Charles University, Faculty of Medicine in Hradec Králové, University Hospital Hradec Králové, Czech Republic

* Corresponding author: 2nd Department of Internal Medicine – Gastroenterology, Sokolská 581, 500 05 Hradec Králové, Czech Republic; e-mail: peterove@lfhk.cuni.cz

Received: 13 December 2017

Accepted: 27 April 2018

Published online: 2 July 2018

Acta Medica (Hradec Králové) 2018; 61(1): 8–16

<https://doi.org/10.14712/18059694.2018.17>

© 2018 The Authors. This is an open-access article distributed under the terms of the Creative Commons Attribution License (<http://creativecommons.org/licenses/by/4.0>), which permits unrestricted use, distribution, and reproduction in any medium, provided the original author and source are credited.

INTRODUCTION

Exhaled breath condensate (EBC) is a biological fluid that consists mainly of water, but it also contains small droplets of airway lining fluid (36). Condensate carries molecules <65 kDa (25). EBC contains both, volatile and non-volatile compounds (35). Adenosine, ammonia, hydrogen peroxide, isoprostanes, leukotrienes, nitrogen oxides, peptides, cytokines belong to the compounds detected in EBC (42). In the clinical setting, non-volatile components, such as cytokines, are used for diagnostics and for monitoring of disease progression (87, 61, 27).

First reports on the EBC collection were published in early 1980s. The report on the EBC collection from the 1990s shows that the condensate was obtained by passing expired gas through tubing submerged in an ice-water bath (7). The first EBC studies documented, that the exhaled breath condensate test is simple, non-invasive and easy to perform. Homemade and commercially manufactured condensers are available today. Various homemade devices have been described, for example a Teflon or a Polypropylen tube, dipped in a bucket filled with ice, a double glass layer container or a device, where exhaled air condensation takes place between the two layers (70, 83, 102). Commercially manufactured condensers are also available, for example EcoScreen, Turbodeccs, ANACON or RTube (90, 26, 85, 14).

Nowadays, there is an increased interest in non-invasive diagnostics and investigation. Collection of EBC fulfils requirements of a non-invasive, repeatable test and thus applicable in the pediatric population (20, 88, 100) and in adult patients, especially in those, who have to control parameters daily. EBC has the potential to become a routine method used for diagnostics, mainly for lung diseases such as bronchial asthma (98, 33, 92, 16, 74), cystic fibrosis (101), idiopathic pulmonary fibrosis (82), bronchiectasia (64), tuberculosis (69), lung carcinoma (2, 46), acute lung injury and acute respiratory distress syndrome (19), chronic obstructive pulmonary disease (59), scleroderma with pulmonary involvement (38, 67), sleep apnea syndrome (18, 89), silicosis (77, 60) and other occupational lung diseases (24, 76, 75, 80, 92). Recently, EBC has been used in monitoring gastrointestinal diseases, such as gastroesophageal reflux disease (91, 81, 39, 58), inflammatory bowel disease (56, 52, 44), coeliac disease (5, 43). Other studies were carried out to monitor systemic sclerosis (28, 93), liver diseases (6), abdominal surgery (66, 84, 65), obese population (13), impacts of oxidative stress (78, 94, 63) or for toxicity screening (34, 79, 57).

If the breath is captured and analyzed correctly, it can be used to provide information of the current health status with a potential to predict future outcomes progression of the disease (50). Nowadays, the PubMed (at <https://www.ncbi.nlm.nih.gov/pubmed>) registers more than 1,300 scientific papers on EBC. However, several methodological issues, including standardization of EBC technique and validation of analytical methods, need to be addressed before this approach can be considered and taken into real practice. EBC composition may be influenced the time of exhalation, condenser temperature, use of nose clips, temperature and duration of condensate storage, saliva con-

tamination, smoking, eating, drinking of coffee may influence composition of EBC. The American Thoracic Society and European Respiratory Society developed guidelines for EBC collection and measurement of exhaled biomarkers, to suggest recommendations on the possible use and limits of exhaled biomarkers and to highlight those areas where further research is required (42).

Nevertheless, the major disadvantage and shortcoming of the EBC is lack of reliable and reproducible standardization of the method (37, 70, 54).

The aim of this study was to introduce our own method, to search for possible standardization and to obtain our own initial experience in healthy volunteers.

METHODS

SUBJECTS

Thirty healthy volunteers between 25–69 years of age were included in the study. The volunteers were the staff of the Faculty Hospital and the Faculty of Medicine of the Charles University in Hradec Králové. The exclusion criteria were the history of chronic lung disease or other serious chronic illness or respiratory infection within 2 weeks preceding the study. The group contained 14 smokers and 16 non-smokers. The project was carried out according to the Declaration of Helsinki, and was approved by the Ethics Committee (201706S11P) of the University Hospital in Hradec Králové. All participants signed an informed consent.

CONDENSATION OF EXHALED BREATH

The condenser EcoScreen (Jaeger, Hoechberg, Germany) is a system in which a mouthpiece with a one-way valve and a refrigerated collecting system are connected to a power supply by an extendable arm. Due to the function of the valve (which is connected to the mouthpiece), inspiratory and expiratory air are separated. The collecting system is connected to the valve block and is placed in a cooling thermoblock. During exhalation, air flows through the lamellar condenser, becomes liquid, and drops into the collecting vial.

All parts of the collection kit were rinsed with ethanol and deionised water and were air dried before each use. The subjects rinsed their mouth with infant water ($\text{Cl}^- < 5 \text{ mg/L}$) with a defined composition. The subject did not smoke, did not eat and did not drink coffee or sweet lemonade at least one hour before sampling. The subjects were not exposed to increased physical activity for at least 30 minutes before sampling. The sampling occurred between 8:00 and 11:00 a.m. The EcoScreen was cooled to -10°C , based on the information provided by the manufacturers. EBC was collected during 10 minutes of exhalation. After 10 minutes of quiet breathing, 1–3 mL of EBC were collected from adult individuals. Volume of EBC is proportional to the total exhaled volume and breathing frequency. EBC samples were immediately transferred to polypropylene tubes and were frozen at -80°C .

In order to examine repeatability of the measurements over a moderate period of time, the collection of EBC was repeated after two weeks.

DENSITY DETERMINATION

Total amount of 500 μL of EBC was transferred by a validated pipette to a polypropylene tube of defined weight. Thereafter, the condensate tube was weighed on Sartorius analytical balances (Germany). Accuracy of measurement was at 0.01 mg and was repeated three times. The measurement was run at 25 °C.

PROTEIN DETERMINATION

Protein content was determined with a diagnostic reagent for quantitative *in vitro* determination of Bio-La-Test Total Protein kit (Erba Lachema, Czech Republic). Named values were verified by determination Bicinchoninic Acid Protein Assay Kit (Sigma-Aldrich). The measurement was run at 37 °C and was repeated three times.

UREA DETERMINATION:

Urea content was determined with a diagnostic reagent for quantitative *in vitro* determination of Bio-La-Test Urea kit (Erba Lachema, Czech Republic). The measurement was run at 37 °C and was repeated three times.

CHLORIDE DETERMINATION

Chloride content was determined with a Ion-selective chloride electrode (Fisher Scientific, Czech Republic). The measurement was run at 25 °C and was repeated three times.

PH DETERMINATION

All samples were deaerated in an ultrasonic bath. pH were determined with a pH electrode (Fisher Scientific, Czech Republic). The measurement was run at 25 °C and was repeated three times.

STATISTIC ANALYSIS

Results had normal distribution and therefore are presented as mean \pm SD or median (interquartile range). Data

obtained were tested statistically by means of non-paired t-test. All statistics was performed using SigmaStat software (Jandel Scientific, Eckhardt, Germany, Version 3.1).

RESULTS

SUBJECTS

Thirty healthy volunteers, 24 females and 6 males, were included in the study. The mean age of the female and male subjects was comparable (40.4 years, range: 25–58 and 39.7 years, range: 28–69, $P = 0.93$). The group included 14 smokers and 16 non-smokers. The proportions of smokers among females and males were 10/24 (42%) and 4/6 (67%), respectively ($P = 0.38$). The mean age of non-smokers and smokers did not differ (40.8 years, range: 25–58 vs. 39.6 years, range: 25–69, $P = 0.93$).

TWO-WEEK REPEATABILITY OF EBC MEASUREMENTS

The repeated measures analysis of variance was used to calculate the average intra-individual and inter-individual coefficients of variation of duplicate measurements performed two weeks apart as well as the intraclass correlation coefficient (Table 1). The mean intra-individual variabilities are considerable for the concentration of total protein, chloride and urea. On the contrary, the measurements of density and pH shows the lowest $\%CV_{intra}$. The intraclass correlation coefficient was good for pH (ICC = 0.81) and moderate for urea measurement (ICC = 0.52), whereas its negative values indicated that the test-retest variability ($\%CV_{intra}$) of density and total protein was higher than the interindividual variability ($\%CV_{inter}$) (Table 1). The repeatability of EBC pH and urea measurements is visualized with the help of Bland-Altman plots in Figure 1.

DENSITY

Density of EBC sample was 1007.2 ± 4.7 g/L (Table 1). Density of EBC was not dependent on smoking, gender or age of subjects. There was no statistically significant differ-

Tab. 1 Descriptive statistic of measured analytes and physical quantity.

	Density (g/L)	pH	Total Protein ($\mu\text{g}/\text{mL}$)	Chlorides (mmol/L)	Urea ($\mu\text{mol}/\text{L}$)
Mean \pm SD	1007 \pm 4.7	6.8 \pm 0.8	1.6 \pm 1.2	3.1 \pm 1.8	199 \pm 156
SD/Mean (%)	0.5	11.5	74.8	58.0	77.2
Median	1007	7.0	1.3	3.4	173
IQR	1004–1010	6.1–7.4	0.7–2.4	1.2–4.6	83.9–291
Range	996–1016	5.5–8.1	0.1–4.5	0.4–6.2	1.0–610
CV_{intra} (%)	1.5	5.3	61.2	57.7	61.3
CV_{inter} (%)	1.2	12.0	52.0	62.4	88.6
ICC	-0.06	0.81	-0.19	0.20	0.52

The descriptive statistics of measured analytes and physical quantity were calculated from the results of second measurements; SD – standard deviation, IQR – interquartile range. The CV_{intra} (%) and CV_{inter} (%) refer to the mean intra-individual and inter-individual coefficients of variation of duplicate measurements performed two weeks apart; ICC – intraclass correlation coefficient of repeated measurements.

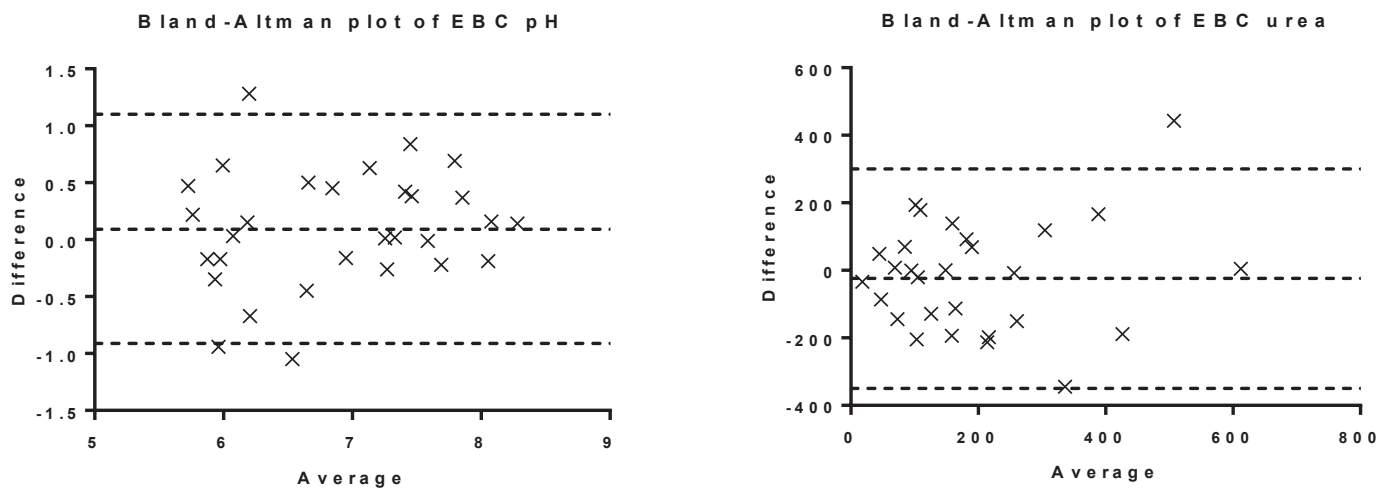


Fig. 1 The repeatability of EBC pH and urea measurements between visits 1 and 2 separated by two weeks. Bland Altman difference vs. average plots with the mean difference and 95% limits of agreement visualized as the broken lines.

Tab. 2 Pearson Product Moment Correlation between variables of interest.

		Age	Density	Chlorides	pH	TP	Urea
Age	r2	x	0.12	0.12	0.10	-0.05	-0.02
	P	x	0.52	0.54	0.58	0.78	0.80
Density	r2	-	x	0.07	-0.19	0.11	0.05
	P	-	x	0.73	0.31	0.55	0.41
Cl-	r2	-	-	x	0.16	-0.18	-0.22
	P	-	-	x	0.40	0.36	0.25
pH	r2	-	-	-	x	-0.33	0.013
	P	-	-	-	x	0.08	0.95
TP	r2	-	-	-	-	x	0.013
	P	-	-	-	-	x	0.95

Coefficients of determination and two-tailed P-values are listed. The existence of correlation was not proved between any of the pairs of variables ($P > 0.05$).

Tab. 3 Univariate analyses of the effects of smoking, age and gender on measured analytes and physical quantity.

	Density (g/L)	pH	Total Protein ($\mu\text{g/mL}$)	Chlorides (mmol/L)	Urea ($\mu\text{mol/L}$)
Smokers, N = 14	1008 \pm 3.4	6.2 \pm 0.5	1.6 \pm 1.5	2.8 \pm 2.0	229 \pm 178
Nonsmokers, N = 16	1006 \pm 5.7	7.4 \pm 0.5	1.9 \pm 1.2	3.4 \pm 1.7	172 \pm 134
P	0.32	< 0.001	0.13	0.41	0.33
Younger (25-40 yr), N = 14	1008 \pm 4.9	6.9 \pm 0.8	1.6 \pm 1.5	3.2 \pm 2.1	227 \pm 181
Older (41-70 yr), N = 16	1007 \pm 4.8	7.0 \pm 0.8	1.3 \pm 1.2	3.0 \pm 1.7	174 \pm 131
P	0.60	0.37	0.82	0.79	0.36
Women, N = 24	1007 \pm 5.0	6.9 \pm 0.8	1.5 \pm 0.9	3.1 \pm 1.9	164 \pm 125
Men, N = 6	1009 \pm 2.8	6.5 \pm 0.7	2.1 \pm 2.1	3.2 \pm 1.7	336 \pm 201
P	0.19	0.25	0.26	0.95	< 0.02

ence between non-smokers and smokers, between females and males and between age groups (Table 3). There were no significant relationships between density and other investigated parameters (Table 2).

PH

EBC pH was 6.8 ± 0.8 (Table 1). pH was dependent on smoking (Figure 2). EBC pH in smokers was lower than in non-smokers. Gender and age of subjects did not influ-

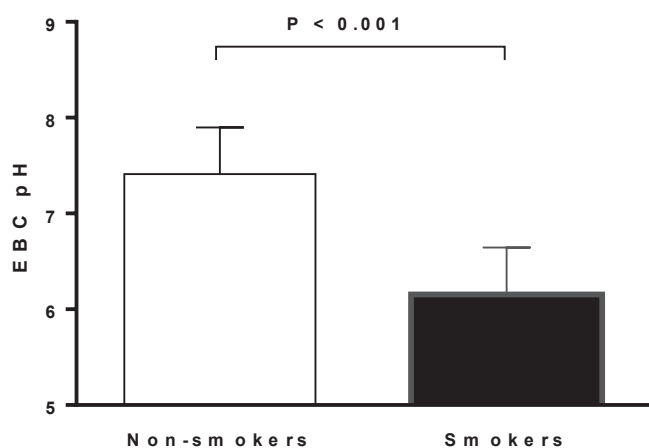


Fig. 2 Exhaled breath condensate pH in non-smokers and smokers. Each bar represents mean \pm SD.

ence pH values (Table 3). There were no significant relationships between pH and other investigated parameters or physical quantity (Table 2).

TOTAL PROTEIN

Total protein concentration were $1.6 \pm 1.2 \mu\text{g/mL}$ (Table 1). Our results show that total protein level is not dependent on smoking, gender and age of subjects. There were no statistically significant differences between non-smokers and smokers, between females and males and between age groups (Table 3). There were no significant relationships between total protein levels and other investigated parameters (Table 2).

CHLORIDE

Chloride ion concentration in EBC samples was $3.1 \pm 1.8 \text{ mmol/L}$ (Table 1). Chloride content was not dependent on smoking, gender and age of subjects. There were no statistically significant differences between non-smokers and smokers, females and males and between age groups (Table 3). There were no significant relationships between chloride ion levels and other investigated parameters (Table 2).

UREA

Urea concentration was $199 \pm 156 \mu\text{mol/L}$ (Table 1). Urea levels were dependent on gender (Figure 3). Urea concentration in females was lower than in males. Smoking and age do not have any impact on urea levels (Table 3). There were no significant relationships between urea levels and other investigated parameters or physical quantity (Table 2).

DISCUSSION

First attempts on breath diagnostics go back to Hippocrates who described foetor ex ore and foetor hepaticus in his treatise on breath smell analysis. The modern era of breath testing was initiated in 1971, when Pauling analyzed volatile organic compounds from breath trapped in

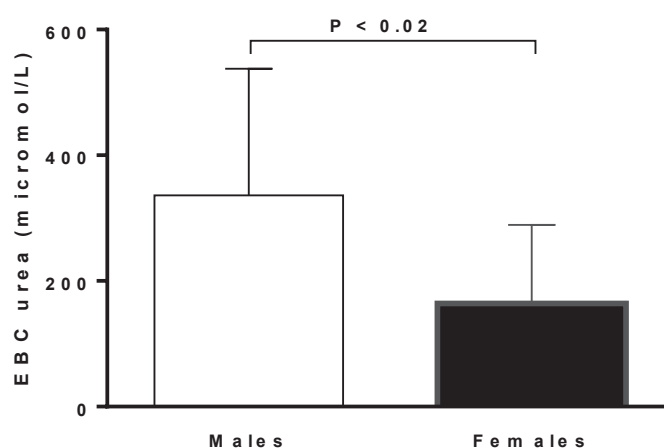


Fig. 3 Concentration of urea in the breath condensate exhaled by men and women. Each bar represents mean \pm SD.

a cooled stainless steel tube and found out that normal human breath contains more than 250 different volatile organic compounds (73, 54). At present, breath analysis is divided into two main directions. The first area of breath analysis deals with the detection of volatile organic compounds. The second areas looks into the aqueous part of breath, which contains mainly non-volatile compounds and water soluble volatiles. There is a lot of studies with both exhaled air analysis and/or, EBC (8, 72).

EBC represents one of the most accessible biological materials, which can be obtained by a non-invasive way. Yet, lack of reliable and reproducible standardization of the method is the major problem at present. Despite multiple articles having been published on EBC, there is no clear consensus at present on whether the analysis of EBC can provide a definite diagnosis of the diseases. There seems to be a high risk of pre-analytical and analytical errors and based on this, interpretation of EBC biomarkers should be taken with a lot of precaution.

There are numerous possible source of pre-analytical errors can be miscellaneous. Collection devices are an important source of variability of EBC biomarkers (86, 40, 21). The other principal factors of variability include cooling temperature (26) and condenser materials (86). Diet, smoking, medication and physical activity influenced EBC results (55, 15, 10, 9). Use of a nose clip is another unsolved question. When using a nose clip, the subject is forced to exhale only through the mouth, preventing thus accidental exhalation through the nose. Yet, the use of a nose clip may affect composition of EBC (95). Currently, there are devices developed by Loccioni Gruppo Humancare (Angeli di Rosora, Italy) which help to assess collection parameters, when the EBC is being obtained from human individuals. These devices provide continuous visual feedback to the subjects to control breathing patterns (99).

The method of determination may be the source of variability in the analytical phase. EBC can be analysed for example by ionex chromatography (47), plasma mass spectrometry (1), Liquid chromatography-mass spectrometry (48) or Polymerase chain reaction (62). We decided to use colorimetric assays and ion-selective electrodes in our study. The possible sources of variability errors are given for the relevant analytes and physical quantities.

The aim of our current study was to search for markers that could serve as a standard that several markers could be related to. Investigated the following parameters: density, pH, total protein level, chloride level and urea level. Some authors suggested that data normalization to the internal control is not necessary, because the levels of analytes during the disease increase many times (17, 23). Carter and colleagues have different view on normalization. Their study showed that standardization should be specific for each biomarker, as a more general model would not optimize collection of all compounds (21).

Our results showed that the density of EBC could be used for standardization. Density meets the requirements in the sense, that it reaches almost the same value across the across the different EBC samples as well as a good test-retest reproducibility of the result. It is not influenced by smoking, gender or age of subjects. Condensed water vapour enriched with trace amounts of volatile and non-volatile components is the major component of the EBC (99, 3). Therefore, the EBC density is close to 1 g/mL and the other dissolved minor components do not change the density. The larger content of dissolved volatile compounds such as ammonia (53) or air trapping in the sample would decrease density. Thus, density could help to compensate for the influence of such factors during sampling but it will unlikely fulfill all expectations for an internal standard. Namely, density is unrelated to the efficiency of the transfer of a particular molecule/ion into exhaled air and, to the completeness of its trapping during cooling.

The interpretation of EBC pH values is complex. EBC pH reflects acidity of the airway lining fluid. However, its value is from a part affected by volatile airway acids (CO_2) and bases (NH_3) which show a variable content upon standing of the EBC sample. The attempts to eliminate CO_2 as a confounding factor included either its removal from the sample by deaeration using an inert gas or saturation of the sample with CO_2 to a stable pH (41). In our study, we used deaeration using ultrasonic baths that secures that CO_2 was removed. Vaughan et al were able to document that EBC pH reflects lung homeostasis. The pH of the airway in health has been reported to be slightly alkaline while acidification of EBC occurs during disease states (96). The pH also depends on temperature of sampling and volume of NH_4^+ . EBC collected at -70°C were more acidic than those collected at -20°C (26) We assume that we eliminated this variability by using Ecosreen and followed the same conditions in all sampling. The literature shows that pH is influenced by diet (55). Ćalušić et al showed that consuming a standardized meal constituting 101.3 g of water, 34 g of protein, 11.2 g of fat, and 47.3 g of saccharides has no effect on pH (15). Hunt et al. found EBC pH decreased significantly after 50 ml sweet limonade and returned to baseline after 15 min (Hunt et al. 2006). We have eliminated the effect of food and beverages by avoiding least one hours before the sampling. The subjects were also not exposed to increased physical activity for at least 30 minutes before sampling. Bikov et al. found that following exercise EBC pH decreased in exercise-induced bronchoconstriction positive group although in healthy subjects this

decline was not demonstrated (11). Thus, amount of NH_4^+ found in the EBC reflects the contamination with salivary NH_3 , some of which is derived from bacterial degradation of urea (29). Volume NH_4^+ can be reduced by washing the mouth with infant water.

Smoking is another factor which influences pH. According to several studies, EBC pH may be lower in smokers compared to non-smokers (4, 51, 40). We confirmed this, too. The measurement of pH with a glass electrode is technically simple. The intraclass correlation coefficient of EBC pH was the highest of all analytes examined in this study. However, the influence of general factors on the EBC pH including the unstable content of volatile acids/bases, hydration of the airways, smoking, exercise-induced bronchoconstriction etc., precludes its use for standardization of the EBC measurements.

We also revealed, that there was a substantial variability in total protein concentration among investigated subjects. Our results are consistent with a study by Bloemen et al. Their study showed that total protein concentration of EBC differed significantly between healthy individuals. Unlike we did, she showed a correlation between the age of subjects and total protein concentration (12). The variability in total protein values might be caused by protease activity (49). The addition of protease inhibitors may further prevent degradation of proteins, however, protease inhibitors can interfere with protein analysis. EBC storage also plays its role. Storage in polyethylene tubes minimizes protein adhesion. (22). Elevated inflammatory markers in respiratory disease increase total protein levels in EBC (68). Type of material of the inner part of the condensers may also play its role. Ecosreen had greater albumin retention compared to glass or Teflon coatings (86).

Our results showed that chlorides are not suitable for standardization. This observation is consistent with the hypothesis that EBC chloride correlates with plasma chloride levels (30). Physical exercise can alter ion regulation by increasing chloride secretion to a significant and similar degree compared to the individuals with cystic fibrosis (97). EBC of patients with chronic persistent cough is more acidic and has lower chloride levels than EBC of non-coughing healthy subjects (71). We did not find any correlation between pH and chloride levels.

Urea concentrations in the EBC are quite low and more variable than the other evaluated parameters, i.e. density and pH. It is believed that the EBC urea value correlates with plasma urea levels (32) as well as chloride levels. NH_4^+ can also interfere with urea analysis (31).

CONCLUSIONS

EBC analysis has a potential become a safe and a non-invasive diagnostic test, not only for lung diseases. In the future it could replace some of more invasive methods. In order to address the issues regarding standardization, it is necessary to consider the matter of collection devices and techniques, modes and conditions. Standardization needs to be specific for each individual biomarker, with future investigations focusing on optimal collection.

ACKNOWLEDGEMENTS

This work was supported by the project PROGRES Q40-15 and Q40-01 (from Charles University).

REFERENCES

- Aherrera A, Olmedo P, Grau-Perez M et al. The association of e-cigarette use with exposure to nickel and chromium: A preliminary study of non-invasive biomarkers. *Environmental Research* 2017; 19: 313–20.
- Ahmed N, Bezabeh T, Ijare OB et al. Proton Magnetic Resonance Spectroscopy (1H MRS) of Sputum and Exhaled Breath Condensate: A Noninvasive Tool for Lung Cancer Screening. *Traditional Journal of Radiation Oncology* 2016; 96: E432.
- Aksenov AA, Zamuruyev KO, Pasamontes A et al. Analytical methodologies for broad metabolite coverage of exhaled breath condensate. *Journal of Chromatography B* 2017; 1061–1062: 17–25.
- Antus B, Barta I, Kullmann T et al. Assessment of exhaled breath condensate pH in exacerbations of asthma and chronic obstructive pulmonary disease: A longitudinal study. *American Journal of Respiratory and Critical Care Medicine* 2010; 182: 1492–7.
- Apra E, Cappellin L, Gasperi F et al. Application of PTR-TOF-MS to investigate metabolites in exhaled breath of patients affected by coeliac disease under gluten free diet. *Journal of Chromatography B* 2014; 966: 208–13.
- Augusto VS, Rodrigues AJ, C Silveira AP et al. Exhaled and plasma nitrite: a comparative study among healthy, cirrhotic and liver transplant patients. *Arquivos De Gastroenterologia* 2014; 51: 16–20.
- Baldwin SR, Grum CM, Boxer LA et al. Oxidant activity in expired breath of patients with adult respiratory distress syndrome. *The Lancet* 1986; 4: 11–3.
- Balint B, Donnelly LE, Hanazawa T, Kharitonov SA, Barnes PJ. Increased nitric oxide metabolites in exhaled breath condensate after exposure to tobacco smoke. *Thorax* 2001; 56: 456–61.
- Barreto M, Villa MP, MD, Olita C et al. 8-Isoprostane in Exhaled Breath Condensate and Exercise-Induced Bronchoconstriction in Asthmatic Children and Adolescents. *Chest Journal* 2009; 135: 66–73.
- Biernacki WA, Kharitonov SA, Barnes PJ. Increased leukotriene B4 and 8-isoprostane in exhaled breath condensate of patients with exacerbations of COPD. *Thorax* 2003; 58: 294–8.
- Bikov A, Galffy G, Tamasi L et al. Exhaled breath condensate pH decreases during exercise-induced bronchoconstriction. *R espirology* 2014; 19: 563–9.
- Bloemen K, Lissensa G, Desagerb K, Schoetersa G. Determinants of variability of protein content, volume and pH of exhaled breath condensate. *Respiratory Medicine* 2007; 101: 1331–7.
- Bodini A, Tenero L, Sandri M et al. Serum and exhaled breath condensate leptin levels in asthmatic and obesity children: a pilot study. *Journal of Breath Research* 2017; 11: 046005.
- Caglieri A, Goldoni M, Acampa O et al. The Effect of Inhaled Chromium on Different Exhaled Breath Condensate Biomarkers among Chrome-Plating Workers. *Environmental Health Perspectives* 2006; 114: 542–46.
- Čalušić AL, Varnai VM, Macan J. Acute effects of smoking and food consumption on breath condensate pH in healthy adults. *Experimental Lung Research* 2011; 37: 92–100.
- Cap P, Maly M, Pehel F, Pelikan Z. Exhaled leukotrienes and bronchial responsiveness to methacholine in patients with seasonal allergic rhinitis. *Annals of Allergy, Asthma & Immunology* 2009; 102: 103–9.
- Carpagnano GE, Carratú P, Gelardi M et al. Increased IL-6 and IL-4 in exhaled breath condensate of patients with nasal polyposis. *Monaldi Archives for Chest Disease* 2009; 71: 3–7.
- Carpagnano GE, Spanevello A, Sabato R et al. Exhaled pH, exhaled nitric oxide, and induced sputum cellularity in obese patients with obstructive sleep apnea syndrome. *Translational Research* 2008; 151: 45–50.
- Carpenter CT, Price PV, Christman BW. Exhaled Breath Condensate Isoprostanes Are Elevated in Patients With Acute Lung Injury or ARDS. *Chest* 1998; 114: 1653–59.
- Carraro S, Giordano G, Reniero F et al. Asthma severity in childhood and metabolomic profiling of breath condensate. *Allergy* 2013; 68: 110–17.
- Carter SR, Davis CS, Kovacs EJ. Exhaled breath condensate collection in the mechanically ventilated patient. *Respiratory Medicine* 2012; 106: 601–13.
- Conrad DH, Goyette J, Thomas PS. Proteomics as a Method for Early Detection of Cancer: A Review of Proteomics, Exhaled Breath Condensate, and Lung Cancer Screening 2008; 23: 78–84.
- Corradi M, Folesani G, Andreoli R et al. Aldehydes and glutathione in exhaled breath condensate of children with asthma exacerbation. *American Journal of Respiratory and Critical Care Medicine* 2003; 167: 395–9.
- Corradi M, Gergelova P, Mutti A. Use of exhaled breath condensate to investigate occupational lung diseases. *Current Opinion in Allergy and Clinical Immunology* 2010; 10: 93–8.
- Cunningham S, McColm JR, Pei Ho L, Greening AP, Marshal TG. Measurement of inflammatory markers in the breath condensate of children with cystic fibrosis. *The European Respiratory Journal* 2000; 15: 955–7.
- Czebe K, Barta I, Antus B et al. Influence of condensing equipment and temperature on exhaled breath condensate pH, total protein and leukotriene concentrations. *Respiratory Medicine* 2008; 102: 720–25.
- Dalaveris E, Kerenidi T, Katsabeki-Katsafli A et al. VEGF, TNF- α and 8-isoprostane levels in exhaled breath condensate and serum of patients with lung cancer. *Lung Cancer* 2009; 64: 219–25.
- Edmé JL, Tellart AS, Launay D et al. Cytokine concentrations in exhaled breath condensates in systemic sclerosis. *Inflammation Research* 2008; 57: 151–6.
- Effros RM, Casaburi R, Su J et al. The effects of volatile salivary acids and bases on exhaled breath condensate pH. *American Journal of Respiratory and Critical Care Medicine* 2006; 173: 386–92.
- Effros RM, Hoagland KW, Bosbous M et al. Dilution of respiratory solutes in exhaled condensates. *American Journal of Respiratory and Critical Care Medicine* 2002; 165: 663–9.
- Effros RM. Do low exhaled condensate NH₄⁺ concentrations in asthma reflect reduced pulmonary production? *American Journal of Respiratory and Critical Care Medicine* 2003; 167: 91–2.
- Esther CR Jr, Boysen G, Olsen BM et al. Mass spectrometric analysis of biomarkers and dilution markers in exhaled breath condensate reveals elevated purines in asthma and cystic fibrosis. *American Journal of Physiology. Lung Cellular and Molecular Physiology* 2009; 296: 1987–93.
- Fulcher YG, Fotso M, Chang CH et al. Noninvasive Recognition and Biomarkers of Early Allergic Asthma in Cats Using Multivariate Statistical Analysis of NMR Spectra of Exhaled Breath Condensate. *PLOS ONE* 2016; 11: e0164394.
- García-Gómez D, Bregy L, Nussbaumer-Ochsne Y et al. Detection and Quantification of Benzothiazoles in Exhaled Breath and Exhaled Breath Condensate by Real-Time Secondary Electrospray Ionization–High-Resolution Mass Spectrometry and Ultra-High Performance Liquid Chromatography. *Environmental Science & Technology* 2015; 49: 12519–24.
- Gasparič J, Hyšpler R, Tichá A. Exhaled breath and metabolism disorders (in Czech). *Vesmír* 2004; 83: 283–285.
- Goldoni M, Caglieri A, Andreoli R et al. Influence of condensation temperature on selected exhaled breath parameters. *BMC Pulmonary Medicine* 2005; 5: 1–9.
- Grob NM, Aytakin M, Dweik RA. Biomarkers in exhaled breath condensate: a review of collection, processing and analysis. *Journal of Breath Research* 2008; 2: 1752–55.
- Guillen-Del Castillo A, Sánchez-Vidaurre S, Simeón-Aznar C, et al. FRI0442 Prognostic Role of Exhaled Breath Condensate in Patients with Pulmonary Involvement Associated to Systemic Sclerosis. *Annals of the Rheumatic Diseases* 2015; 74: 587.
- Heffler E, Crimi M, Brussino L et al. Exhaled breath condensate pH and cysteinyl leukotriens in patients with chronic cough secondary to acid gastroesophageal reflux. *Journal of Breath Research* 2017; 11: 016002.
- Hoffmeyer F, Raulf-Heimsoth M, Harth V, Bünger J, Brüning T. Comparative analysis of selected exhaled breath biomarkers obtained with two different temperature-controlled devices. *BMC Pulmonary Medicine* 2009; 9: 48.
- Horváth I, Barnes PJ, Loukides S, et al. A European Respiratory Society technical standard: exhaled biomarkers in lung disease. *Eur Respir J* 2017; 49(4).
- Horváth I, Hunt J, Barnes PJ. Exhaled breath condensate: methodological recommendations and unresolved questions. *The European Respiratory Journal* 2005; 26: 523–48.
- Hrynjuk A, Ross BM. A preliminary investigation of exhaled breath from patients with celiac disease using selected ion flow tube mass spectrometry. *Journal of Gastrointestinal and Liver Diseases* 2010; 19: 15–20.
- Huang Y, Lemberg DA, Day AS et al. Markers of inflammation in the breath in paediatric inflammatory bowel disease. *Gastroenterology* 2014; 59: 505–10.

45. Hunt J, Yu Y, Burns J et al. Identification of acid reflux cough using serial assays of exhaled breath condensate pH. *Cough* 2006; 2: 3.
46. Chen JL, Lv XD, Ma H2, Chen JR, Huang JA. Detection of cancer embryo antigen and endothelin-1 in exhaled breath condensate: A novel approach to investigate non-small cell lung cancer. *Molecular and Clinical Oncology* 2016; 5: 124-8.
47. Chladkova J, Krcmova I, Chladek J et al. Validation of nitrite and nitrate measurements in exhaled breath condensate. *Respiration* 2006; 73: 173-9.
48. Jackson TC, Zhang YV, Sime PJ, Phipps RP, Kottmann RM. Development of an accurate and sensitive method for lactate analysis in exhaled breath condensate by LC MS/MS. *Journal of Chromatography B* 2017; 1061-2: 468-73.
49. Karakoc GB, Inal A, Yilmaz M, Altintas DU, Kendirli SG. Exhaled breath condensate MMP-9 levels in children with bronchiectasis. *Pediatric Pulmonology* 2009; 44: 1010-6.
50. Kim KH, Jahan SA, Kabir E. A review of breath analysis for diagnosis of human health. *Trends in Analytical Chemistry* 2012; 33: 1-8.
51. Koczulla AR, Noeske S, Herr C et al. Acute and chronic effects of smoking on inflammation markers in exhaled breath condensate in current smokers. *Respiration*. 2010; 79: 61-7.
52. Krenke K, Peradzyńska J, Lange J et al. Inflammatory cytokines in exhaled breath condensate in children with inflammatory bowel diseases. *Pediatric Pulmonology* 2014; 49: 1190-5.
53. Krishnan ST, Devadhasan JP, Kim S. Recent analytical approaches to detect exhaled breath ammonia with special reference to renal patients. *Analytical and Bioanalytical Chemistry* 2017; 409: 21-31.
54. Kubáň P, Foret F. Exhaled breath condensate: Determination of non-volatile compounds and their potential for clinical diagnosis and monitoring. A review. *Analytica Chimica Acta* 2013; 805: 1-18.
55. Kullmann T, Barta I, Antus B, Horváth I. Drinking Influences Exhaled Breath Condensate Acidity. *Lung* 2008; 186: 263-68.
56. Kurada S, Alkhoury N, Fiocchi C, Dweik R, Rieder F. Review article: breath analysis in inflammatory bowel diseases. *Alimentary Pharmacology and Therapeutics* 2015; 41: 329-41.
57. Ladva CN, Golan R, Greenwald R, et al. Metabolomic Profiles of Plasma, Exhaled Breath Condensate, and Saliva are Correlated with Potential for Air Toxics Detection. *Journal of Breath Research* 2017; JBR-100601.R2.
58. Lee AL, Button BM, Denehy L et al. Exhaled Breath Condensate Pepsin: Potential Noninvasive Test for Gastroesophageal Reflux in COPD and Bronchiectasis. *Respiratory Care* 2015; 60: 244-50.
59. Lee JS, Shin JH, Hwang J-H, Baek JE, Choi B-S. Malondialdehyde and 3-Nitrotyrosine in Exhaled Breath Condensate in Retired Elderly Coal Miners with Chronic Obstructive Pulmonary Disease. *Safety and Health at Work* 2014; 5: 91-6.
60. Leese E, Staffl JF, Carolan VA, Morton J. Exhaled Breath Condensate: A Novel Matrix for Biological Monitoring to Assess Occupational Exposure to Respirable Crystalline Silica. *Annals of Work Exposures and Health* 2017; 61: 902-6.
61. Li Y, Chongsuvivatwong V, Geater A, Liu A. Exhaled breath condensate cytokine level as a diagnostic tool for obstructive sleep apnea syndrome. *Sleep Medicine* 2009; 10: 95-103.
62. Lin X, Wu Z, Fan Y et al. Correlation analysis of surfactant protein A and surfactant protein D with lung function in exhaled breath condensate from lung cancer patients with and without COPD. *Molecular Medicine Reports* 2017; 16: 4948-54.
63. Liu D, Luo G, Luo C et al. Changes in the Concentrations of Mediators of Inflammation and Oxidative Stress in Exhaled Breath Condensate During Liver Transplantation and Their Relations With Postoperative ARDS. *Respiratory care* 2015; 60: 679-88.
64. Loukides S, Horvath I, Wodehouse T, Cole PJ, Barnes PJ. Elevated Levels of Expired Breath Hydrogen Peroxide in Bronchiectasis. *American Journal of Respiratory and Critical Care Medicine* 1998; 158: 991-994.
65. Łuczynańska M, Szkudlarek U, Dziankowska-Bartkowiak B, Waszczykowska E, Kasielski M, Sysa-Jedrzejowska A, Nowak D. Elevated exhalation of hydrogen peroxide in patients with systemic sclerosis. *Eur J Clin Invest* 2003; 33: 274-279.
66. Mahairidou A, Rodopoulou S, Tomos I et al. Exhaled Breath Condensate Acidification Occurs During Surgery for Abdominal Cancer. *Anticancer Research* 2017; 37: 3315-21.
67. Marie-Desvergne C, Dubosson M, Touri L et al. Assessment of nanoparticles and metal exposure of airport workers using exhaled breath condensate. *Journal of Breath Research* 2016; 10: 036006.
68. Moloney ED, Mumby SE, Gajdosci R et al. Exhaled breath condensate detects markers of pulmonary inflammation after cardiothoracic surgery. *American Journal of Respiratory and Critical Care Medicine* 2004; 169: 64-69.
69. Mosquera-Restrepo SF, Caro AC, García LF, Peláez-Jaramillo CA, Rojas M. Fatty acid derivative, chemokine, and cytokine profiles in exhaled breath condensates can differentiate adult and children paucibacillary tuberculosis patients. *Journal of Breath Research* 2017; 11: 016003.
70. Mutlu GM, Garey KW, Robbins RA et al. Collection and Analysis of Exhaled Breath Condensate in Humans. *American Journal of Respiratory and Critical Care Medicine* 2001; 164: 731-7.
71. Niimi A, Nguyen LT, Usmani O, Mann B, Chung KF. Reduced pH and chloride levels in exhaled breath condensate of patients with chronic cough. *Thorax* 2004 Jul; 59: 608-12.
72. Ojoo JC, Mulrennan SA, Kastelik JA, Morice AH, Redington AE. Exhaled breath condensate pH and exhaled nitric oxide in allergic asthma and in cystic fibrosis. *Thorax* 2005; 60: 22-6.
73. Pauling L, Robinson AB, Teranishi R, Cary P. Quantitative Analysis of Urine Vapor and Breath by Gas-Liquid Partition Chromatography. *Proceedings of the National Academy of Sciences* 1971; 68: 2374-6.
74. Peel AM, Crossman-Barnes CJ, Tang J et al. Biomarkers in adult asthma: a systematic review of 8-isoprostane in exhaled breath condensate. *Journal of Breath Research* 2017; 11: 016011.
75. Pelclova D, Barosova H, Kukutschova J et al. Raman microspectroscopy of exhaled breath condensate and urine in workers exposed to fine and nano TiO₂ particles: a cross-sectional study. *Journal of Breath Research* 2015; 9: 036008.
76. Pelclová D, Fenclová Z, Kacer P et al. Increased 8-isoprostane, a marker of oxidative stress in exhaled breath condensate in subjects with asbestos exposure. *Industrial Health* 2008; 46: 484-9.
77. Pelclová D, Fenclová Z, Kačer P et al. 8-isoprostane and Leukotrienes in Exhaled Breath Condensate in Czech Subjects with Silicosis. *Industrial Health* 2007; 45: 766-74.
78. Pelclova P, Zdimal V, Kacer P et al. Oxidative stress markers are elevated in exhaled breath condensate of workers exposed to nanoparticles during iron oxide pigment production. *Journal of Breath Research* 2016; 10: 016004.
79. Pleil JD. Breath biomarkers in toxicology. *Archives of Toxicology* 2016; 90: 2669-82.
80. Radauceanu A, Grzebyk M, Edmé JL et al. Effects of occupational exposure to poorly soluble forms of beryllium on biomarkers of pulmonary response in exhaled breath of workers in machining industries. *Toxicology Letters* 20016; 263: 26-33.
81. Reeder NP, Davis CS, Kovacs EJ, Fisichella PM. The diagnostic value of gastroesophageal reflux disease (GERD) symptoms and detection of pepsin and bile acids in bronchoalveolar lavage fluid and exhaled breath condensate for identifying lung transplantation patients with GERD-induced aspiration. *Surgical Endoscopy* 2014; 28: 1794-800.
82. Rindlisbacher R, Strebel C, Guler S et al. Exhaled breath condensate as a potential biomarker tool for idiopathic pulmonary fibrosis - a pilot study. *Journal of Breath Research* 2017; 12(1): 016003.
83. Robroeks CMHHT, van de Kant KDG, Jöbsis Q et al. Exhaled nitric oxide and biomarkers in exhaled breath condensate indicate the presence, severity and control of childhood asthma. *Clinical and Experimental Allergy* 2007; 37: 1303-11.
84. Rolla G, Fusaro E, Nicola S, Bucca C, Peroni C, Parisi S, Cassinis MC, Ferraris A, Angelino F, Heffler E, Boita M, Brussino L. Th-17 cytokines and interstitial lung involvement in systemic sclerosis. *J Breath Res* 2016; 10: 046013.
85. Romero PV, Rodríguez B, Martínez S et al. Analysis of Oxidative Stress in Exhaled Breath Condensate From Patients With Severe Pulmonary Infections. *Archivos De Bronconeumologia* 2006; 42: 113-9.
86. Rosias PP, Robroeks CM, Kesker A et al. Biomarker reproducibility in exhaled breath condensate collected with different condensers. *The European Respiratory Journal* 2008; 31: 934-42.
87. Sack U, Scheibe R, Wotzel M et al. Multiplex Analysis of Cytokines in Exhaled Breath Condensate. *International Society for Analytical Cytology* 2006; 69A: 169-72.
88. Shahid SK, Kharitonov SA, Wilson NM, Bush A, Barnes PJ. Increased Interleukin-4 and Decreased Interferon- γ in Exhaled Breath Condensate of Children with Asthma. *American Journal of Respiratory and Critical Care Medicine* 2002; 165: 1290-93.
89. Schwarz EI, Engler A, Kohler M. Exhaled breath analysis in obstructive sleep apnea. *Journal Expert Review of Respiratory Medicine* 2017; 11: 631-9.
90. Soyer OU, Dizdar EA, Keskin O, Lilly C, Kalayci O. Comparison of two methods for exhaled breath condensate collection. *Allergy* 2006; 61: 1016-18.
91. Soyer T, Soyer OU, Birben E et al. Pepsin levels and oxidative stress markers in exhaled breath condensate of patients with gastroesophageal reflux disease. *Journal of Pediatric Surgery* 2013; 48: 2247-50.

92. Syslová K, Kačer P, Kuzma M et al. Determination of 8-iso-prostaglandin F2 in exhaled breath condensate using combination of immunoseparation and LC-ESI-MS/MS. *Journal of Chromatography B* 2008; 867: 8–14.
93. Tufvesson E, Bozovic G, Hesselstrand R et al. Increased cysteinyl-leukotrienes and 8-isoprostane in exhaled breath condensate from systemic sclerosis patients. *Rheumatology* 2010; 49: 2322–6.
94. Urs R, Simpson S, Pillow J, Hall H, Clarke M. Exhaled breath condensate: Measuring inflammation and oxidative stress in preterm infants. *European Respiratory Journal* 2016; 48: OA243.
95. Vass G, Huszár E, Barát E et al. Comparison of Nasal and Oral Inhalation during Exhaled Breath Condensate Collection. *American Journal of Respiratory and Critical Care* 2003; 167: 850–5.
96. Vaughan J, Ngamtrakulpanit L, Pajewski TN et al. Exhaled breath condensate pH is a robust and reproducible assay of airway acidity. *The European Respiratory Journal* 2003; 22: 889–94.
97. Wheatley CM, Baker SE, Morgan MA et al. Moderate intensity exercise mediates comparable increases in exhaled chloride as albuterol in individuals with cystic fibrosis. *Respiratory Medicine* 2015; 109: 1001–11.
98. Whitehouse A, Brugha R, Mushtaq N, Dundas I, Grigg J. S64 Eosinophil Cationic Protein And Cytokine Analysis In Exhaled Breath Condensate In Paediatric Asthma. *Thorax* 2014; 69: A36.
99. Winters BR, Pleil JD, Angrish MM et al. Standardization of the collection of exhaled breath condensate and exhaled breath aerosol using a feedback regulated sampling device. *Journal of Breath Research* 2017; 11(4): 047107.
100. Zanconato S, Carraro S, Corradi M et al. Leukotrienes and 8-isoprostane in exhaled breath condensate of children with stable and unstable asthma. *Journal of Allergy and Clinical Immunology* 2004; 113(2): 63.
101. Zang X, Pérez JJ, Jones CM et al. Comparison of Ambient and Atmospheric Pressure Ion Sources for Cystic Fibrosis Exhaled Breath Condensate Ion Mobility-Mass Spectrometry Metabolomics. *American Society for Mass Spectrometry* 2017; 28: 1489–96.
102. Rosias PPR, Dompeling E, Hendriks HJE et al. Exhaled breath condensate in children: Pearls and pitfalls. *Pediatr Allergy Immunol* 2004; 15: 4–19.

Immunohistochemical Expression of CDC7 in Dentigerous Cyst, Odontogenic Keratocyst and Radicular Cyst

Zohreh Jaafari-Ashkavandi¹, Ahmad Alipour Tuyeh², Sepideh Assar^{3,*}

ABSTRACT

CDC7 is a serine/threonine kinase which has an essential role in initiation of DNA proliferation and S phase. It increases the invasion and proliferation in many pathologic lesions. This study aimed to evaluate the expression of CDC7 in the most common odontogenic cysts. We evaluated 17 dentigerous cysts, 18 odontogenic keratocysts (OKC) and 13 radicular cysts immunohistochemically. The mean expression of CDC7 was analyzed using ANOVA and Post-HOC methods. All specimens revealed CDC7 expression. Higher expression of CDC7 in OKC and radicular cyst was shown in comparison to dentigerous cyst ($P < 0.001$), while radicular cyst and OKC groups showed no difference in CDC7 expression ($P = 0.738$). The high expression of CDC7 in OKC suggests that this protein could be related to the higher proliferation rate and invasiveness of OKC. On the other hand, the higher CDC7 expression in radicular cyst may simply be related to inflammation as this cyst is neither aggressive nor invasive.

KEYWORDS

CDC7; dentigerous cyst; odontogenic keratocyst; radicular cyst; immunohistochemistry

AUTHOR AFFILIATIONS

¹ Department of Oral & Maxillofacial Pathology, Shiraz Dental School, Shiraz University of Medical Sciences, Shiraz, Iran

² Shiraz Dental School, Shiraz University of Medical Sciences, Shiraz, Iran

³ Department of Oral & Maxillofacial Pathology, Hormozgan Dental School, Hormozgan University of Medical Sciences, Hormozgan, Bandar-Abbas, Iran

* Corresponding author: Hormozgan University of Medical Sciences, Hormozgan, Bandar-Abbas, Iran; e-mail: se.assar@gmail.com

Received: 23 October 2017

Accepted: 23 March 2018

Published online: 2 July 2018

Acta Medica (Hradec Králové) 2018; 61(1): 17–21

<https://doi.org/10.14712/18059694.2018.18>

© 2018 The Authors. This is an open-access article distributed under the terms of the Creative Commons Attribution License (<http://creativecommons.org/licenses/by/4.0>), which permits unrestricted use, distribution, and reproduction in any medium, provided the original author and source are credited.

INTRODUCTION

Odontogenic cysts are developmental lesions that form because of abnormalities that can occur during tooth development. These lesions are commonly found in routine radiographic examination (1). Dentigerous cyst (DC) is the most common developmental odontogenic cyst that involves about 24% of the epithelium lined cysts of the jaws (2, 3). This slow-growing cyst involves the crown of an unerupted tooth due to changes in the reduced enamel epithelium after completion of amelogenesis that results in aggregation of liquid between the reduced enamel epithelium and tooth crown (2–5). Odontogenic keratocyst (OKC) is one of the common cysts that accounts for about 11% of all developmental odontogenic cysts (6) originating from the remnants of the dental lamina. The OKC has a high growth rate and tendency for invasion and recurrence (7). Because of this aggressive behavior, from 2005 to 2017, the OKC was named keratocystic odontogenic tumor by the World Health Organization (WHO) (8, 9). In 2017, the WHO reverted it to the odontogenic keratocyst as a cystic lesion; hence, there is a debate around the putative neoplastic nature of this lesion (9).

Radicular cyst (RC) is the most common cyst of the oral cavity which originates from the epithelium existing in the periodontal space or forming as a result of pulp necrosis (10–13). This inflammatory cyst usually has a low growth rate and is asymptomatic unless there is acute inflammation in the area (12).

In many instances, the differentiation between different cysts is difficult; thus, finding a diagnostic aid seems necessary. Today, immunohistochemistry (IHC) using appropriate diagnostic or prognostic markers can help the pathologists.

Cell division cycle 7 (CDC7) protein is a serine/threonine kinase which plays a key role in the initiation of DNA replication and regulation of G1/S phase transition (check point of the cell cycle) (14). Different mechanisms of modulation of kinase activity in response to DNA replication stress have been reported. In one hypothesis, CDC7 plays an active role in cell cycle stages, but in another one it is an inactive final target in the cell cycle check-point (15, 16). It seems that overexpression of CDC7 by disabling p53 is related to several cancers and cancer cell lines (15).

Hess and colleagues found that CDC7 expresses in many normal tissues such as placenta, fetal tissues, brain, lung and immune system tissues, but it expresses further in many tumors such as colorectal carcinoma, different types of leukemia, lung carcinoma melanoma and all of their modified cell lines. They concluded that expression of CDC7 may be related to increasing proliferation of some tumors and neoplastic changes in other tumors (17). Bonte et al. studied the presence of CDC7 in certain tumors and normal cells and found that CDC7 protein expression in normal tissues derived from the breast, lung and colon was very low or undetectable, but this protein was overexpressed in about 50% of 62 human tumor cells such as different types of leukemia. Overexpression of CDC7 was shown in primary tumors of the breast, colon and lung, but it was not detected in normal tissues of those areas. They also showed the association between decreasing the

p53 and overexpression of CDC7 and DBF4 in primary breast cancer and cancer cell lines (15). Also, inhibition of CDC7 in the cell lines can lead to stopping of the cell cycle. Thus, inhibition of CDC7 may be useful for the treatment of cancer (15, 16, 18).

There is not any study that has been conducted on evaluation of the expression of CDC7 protein in the odontogenic cysts, so this study aimed to evaluate the immunohistochemical expression of this protein in the most common odontogenic cysts.

MATERIALS AND METHODS

In this cross-sectional study, 17 cases of DC, 18 OKC and 13 RC were included. The samples were obtained from Oral and maxillofacial pathology department of Shiraz University of Medical Sciences (1998–2014). All samples had a definite diagnosis and an adequate epithelial component. Inflamed OKCs and DCs were excluded. Baseline data including the patients' age and gender as well as the location of the lesions were noted according to the patients' medical files.

IHC staining was performed using the Envision Labeled Peroxidase System (DAKO, Carpinteria, CA, USA). All the samples had been fixed in 10% formalin and embedded in paraffin previously. After deparaffinization in xylene, the sections were dehydrated in alcohol and washed in distilled water. Antigen retrieval was done by DAKO cytomation target retrieval solution with PH = 9 during 20 minutes. Internal peroxidase activity was inhibited by H₂O₂ 3%. We used CDC7 (Polyclonal rabbit antibody # 1:50, Gentex, USA) as primary antibody. 3,3'-diaminobenzidine tetrahydrochloride (DAB) was used as chromogen and hematoxylin was applied for background staining.

Basal cell layer of the oral mucosa was used as positive control. For negative control, primary antibody was replaced by PBS (phosphate-buffered saline) solution. The cells with brown nuclei were considered as CDC7 positive. In high power, we counted at least 300 cells in three microscopic fields of each specimen. Samples with CDC7 staining <5%, 5–10% and >10% were considered as low, intermediate and high expression of CDC7, respectively (19). Data were analyzed using SPSS software. ANOVA and Post-HOC tests were used. P value ≤0.05 was considered significant statistically.

RESULTS

The mean ± SD age of the cases was 30.66 ± 10.25 years old (range 12–54 years). Baseline characteristics regarding age, gender and location of the lesions in each group are shown in Table 1.

Nuclear expression of CDC7 in basal and para-basal cell layers was observed in all specimens. In the DC group, the mean of CDC7 expression of cells was 3.47 ± 1.4 and it was limited to the basal cell layer (Fig. 1A). Also in RC, in addition to the basal cell layer, positive staining was observed in the parabasal layer and the mean of expression was 20.6 ± 14.9 (Fig. 1B). In the OKC group, more positive CDC7 cells

were observed in the parabasal layer and basal cell layer showed less staining. The mean of positive staining for OKC was 18.15 ± 8.04 (Fig. 1C).

According to ANOVA test, there was a statistically significant difference among the three groups in CDC7 expression ($P < 0.001$). Post-HOC test showed that positive staining for CDC7 in DC was lower than the two other cysts. ($P < 0.001$ for both group); however, RC and OKC did not reveal any significant difference in staining for CDC7 ($P = 0.738$). CDC7 expression in the three groups was divided into three subgroups: low, medium and high, as illustrated in Table 3. Although most of the DCs showed low expression of CDC7, the cases of OKC and RC revealed a high CDC7 expression rate.

DISCUSSION

In the present study, expression of CDC7 in the most common odontogenic cysts was evaluated. OKC had an aggressive behavior and tendency to high recurrence, but DC and RC showed slow growth and low recurrence. Although the exact mechanism for this difference is unknown, many studies explain that the epithelium of OKC could be involved in its aggressive behavior (2). However, some stromal components are also involved in this behavior (20). The results of this study showed that the expression of CDC7 in OKC and RC was higher than DC with a significant difference. In various studies on the expression of CDC7, the total conclusion was that the increase in the expression of this marker is related to higher proliferation activity, or increase in the aggressiveness of the tumor (15, 17, 21, 22). Its mechanism is phosphorylation of MCM2-7 complex (minichromosomal maintenance 2-7), activating the internal pathway of DNA-Helicase activity and initiating

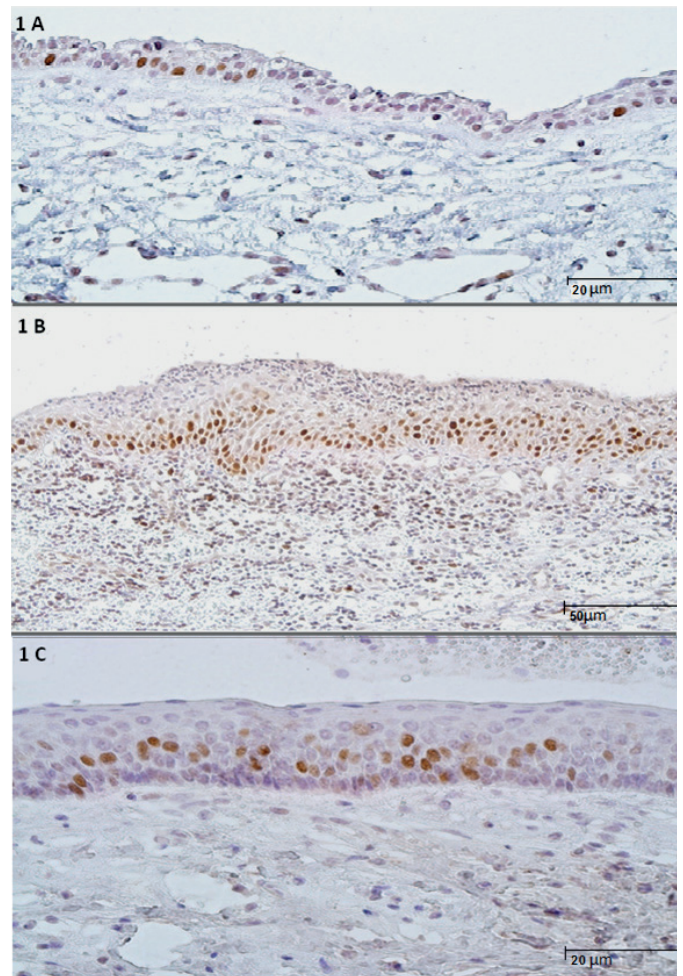


Fig. 1 Nuclear expression of CDC7; 1A: in the basal cell layer of dentigerous cyst ($\times 400$); 1B: in the basal and parabasal classes of Radicular radicular cysts ($\times 200$); 1C: in the parabasal layer of odontogenic keratocyst ($\times 400$).

Tab. 1 Baseline data of all study groups.

Type of Cyst (N)	Age	Male : Female	Maxilla : Mandible
Dentigerous Cyst (17)	29.76 ± 10	14 : 3	7 : 10
Radicular Cyst (13)	35 ± 9.3	8 : 5	8 : 5
Odontogenic Keratocyst (18)	28.2 ± 10.7	8 : 10	4 : 14

Tab. 2 CDC7 expression rate in all study groups.

Type of Cyst (N)	CDC7 (Mean \pm SD)	Min-Max	P-value
Dentigerous Cyst (17)	3.5 ± 1.4	2-6.1	0.000 : vs Rad
			0.000 : vs OKC
Radicular Cyst (13)	20.6 ± 14.9	5.5-49	0.000 : vs D
			0.738 : vs OKC
Odontogenic Keratocyst (18)	18.1 ± 8	9-32.6	0.738 : vs Rad
			0.000 : vs D

Tab. 3 Classification of CDC7 expression in the study.

Type of Cyst(N)	Low	Moderate	igh
Dentigerous Cyst(17)	14	3	-
Radicular Cyst(13)	1	3	9
Odontogenic Keratocyst (18)	-	1	17

the replication of DNA (23); thus, it results in an increase in cell proliferation (24). In previous studies, an increase of MCMs such as MCM2 and MCM 3 was observed in OKC (25); also, many studies have shown an increased proliferative activity of this cyst rather than other odontogenic cysts. MCM positive cells have a high CDC7 activity (25).

CDC7 is used as an initiator for DNA replication in anti-cancer therapeutic purposes. Inhibition of CDC7 expression can cause a destructive S phase and ability to destroy the cancer cells. This feature was recognized by a G1 reverse phase, during inhibition of CDC7 expression that happened by reactivation of the cell cycle checkpoints which were damaged due to cancer (25). In normal cells, a p53-dependent pathway actively inhibits the damaged S phase during the absence of CDC7 kinase, and p53 is essential for maintenance of check-points of the cell cycle (16). Our results reflect the role of CDC7 in higher proliferation of OKC. Moreover, the expression of CDC7 in OKC was seen mostly in the parabasal layer, whereas in other groups it was observed in the basal cell layer. Many studies have observed the suprabasal layer of OKC as the proliferative layer, unlike other odontogenic cysts. In a study, it has been mentioned that the biologic behavior of OKC is due to its proliferative parabasal layer in which Ki-67, p53 and p63 express highly (24).

In this study, we found a higher expression of CDC7 in RC; as proliferation of the RC cells is attributed to the inflammatory process stimuli, we raise the question whether the high CDC7 immunexpression observed in RC might be related to the significant inflammation. Guler and colleagues studied the expression of Ki67 and MCM2 factors, as well as the effects of inflammation on the markers of cell cycle in the cases of dental follicle and odontogenic cysts such as RC, DC and OKC. They concluded that the expression of Ki67 in dental follicle and OKC and expression of MCM2 in RC and OKC were higher statistically. The result of MCM2 in the mentioned study is similar to that of CDC7 expression in our study, which was higher in RC and OKC. They mentioned that there could be a relationship between higher inflammation in RC and higher expression of MCM2 proliferation marker (26).

Among the study groups, DC and OKC showed uniformity in the expression of CDC7; as 82% of DC showed low expression and 94% of OKC revealed high expression of CDC7, but RC had a more scattered staining pattern. Based on these results, the expression of CDC7 could be affected by the amount and type of inflammatory cells. Given that the proliferative markers are used to make a differential diagnosis of pathologic lesions, based on these results, it seems that the effectiveness of this marker in making differential diagnosis in inflamed odontogenic cysts is low. However, further studies focusing on the impact of inflammation are suggested for confirming this point.

CONCLUSION

Based on the present findings, it is concluded that there is a higher expression of CDC7 in odontogenic cysts with higher proliferative activity and higher aggressiveness,

such as OKC. Therefore, it could be a potential prognostic marker. Since the expression of this marker was also high in RC, inflammation appears to contribute to CDC7 expression.

We suggest further studies comparing the RC with inflamed DC and OKC to evaluate the effectiveness of this marker in diagnosis of inflamed lesions and a larger sample size to get a cut-off point for differential diagnosis of the odontogenic cyst.

ACKNOWLEDGEMENTS

The authors thank the Vice-chancellery of Shiraz University of Medical Sciences for supporting this research (Grant #10085). This manuscript is based on the undergraduate thesis of Ahmad Alipour Tuyeh. The authors are also grateful to Dr. Salehi in Dental Research Development Center of Shiraz Dental School for the statistical analysis. The authors would like to thank the research consultation center (RCC) of Shiraz University of Medical Sciences for their invaluable assistance in editing this article.

FUNDING

Vice-chancellery of Shiraz University of Medical Sciences supported this research (Grant #10085).

CONFLICT OF INTEREST

None

ETHICAL APPROVAL

This article has been approved by Ethic committee of Shiraz University of Medical Sciences (Code: IR.SUMS.REC.1394.S762).

REFERENCES

1. Khalifa GA, Shokier H, Abo-Hager E. Evaluation of neoplastic nature of keratocystic odontogenic tumor versus ameloblastoma. *Journal of the Egyptian National Cancer Institute* 2010; 22(1): 61-72.
2. Swetha P, Ramesh K, Madhavan N, Veeravarmal V, Sameera A. Expression of inducible nitric oxide synthase in the epithelial linings of odontogenic keratocyst, dentigerous cyst and radicular cyst: a pathological insight. *Ann Med Health Sci Res.* 2014; 4(4): 583-9.
3. Selvamani M, Donoghue M, Basandi PS. Analysis of 153 cases of odontogenic cysts in a South Indian sample population: a retrospective study over a decade. *Brazilian Oral Research* 2012; 26(4): 330-4.
4. Bhardwaj B, Sharma S, Chitlangia P, Agarwal P, Bhamboo A, Rastogi K. Mandibular Dentigerous Cyst in a 10-Year-Old Child. *International Journal of Clinical Pediatric Dentistry* 2016; 9(3): 281-284.
5. Mohan KR, Natarajan B, Mani S, Sahuthullah YA. An infected dentigerous cyst associated with an impacted permanent maxillary canine, inverted mesiodens and impacted supernumerary teeth. *J Pharm Bioallied Sci* 2013; 5: 135-8.
6. Razavi SM, Khalesi S, Torabinia N. Investigation of clinicopathological parameters alongside with p53 expression in primary and recurrent keratocysticodontogenic tumours. *The Malaysian Journal of Pathology* 2014; 36(2): 105.
7. Bande CR, Prashant M, Sumbh B, Pandilwar P. Prevalence, treatment and recurrence of odontogenic keratocyst in central India. *Journal of Maxillofacial and Oral Surgery* 2010; 9(2): 146-9.

8. Madras J, Lapointe H. Keratocystic odontogenic tumour: reclassification of the odontogenic keratocyst from cyst to tumour. *Texas Dental Journal* 2008; 125(5): 446.
9. Speight P, Devillers P, Li T-J, Odell EW, Wright JM. Odontogenic Keratocyst. In: El-Naggar AK, Ohan JKC, Grandis JR, Takata T, Sloatweg PJ, eds. *WHO Classification of Head and Neck Tumours WHO/IARC Classification of Tumors*, 4th Edition, Volume 9, 2017, pp. 235-236.
10. Vidhale G, Jain D, Jain S, Godhane AV, Pawar GR. Management of Radicular Cyst Using Platelet-Rich Fibrin & Iliac Bone Graft - A Case Report. *J Clin Diag Res*. 2015; 9(6); ZD34-ZD36.
11. Omoregie F, Sede M, Ojo A. Ameloblastomatous change in radicular cyst of the jaw in a Nigerian population. *Ghana Med J* 2015; 49(2): 107-11.
12. Lamba G, Ravi G. Replantation of Displaced Underlying Successor and Marsupialization of Radicular Cyst associated with a Primary Molar. *International Journal of Clinical Pediatric Dentistry* 2015; 8(1): 70.
13. Bava FA, Umar D, Bahseer B, Baroudi K. Bilateral Radicular Cyst in Mandible: An Unusual Case Report. *Journal of International Oral Health: JIOH* 2015; 7(2): 61.
14. Tenca P, Brotherton D, Montagnoli A, Rainoldi S, Albanese C, Santocanale C. CDC7 is an active kinase in human cancer cells undergoing replication stress. *Journal of Biological Chemistry* 2007; 282(1): 208-15.
15. Bonte D, Lindvall C, Liu H, Dykema K, Furge K, Weinreich M. CDC7-Dbf4 kinase overexpression in multiple cancers and tumor cell lines is correlated with p53 inactivation. *Neoplasia* 2008; 10(9): 920-31.
16. Li W, Zhao XL, Shang SQ, Shen HQ, Chen X. Dual Inhibition of Cdc7 and Cdk9 by PHA-767491 Suppresses Hepatocarcinoma Synergistically with 5-Fluorouracil. *Curr Cancer Drug Targets* 2015; 15(3): 196-204.
17. Hess GF, Drong RE, Weiland KL, Slightom JL, Sclafani RA, Hollingsworth RE. A human homolog of the yeast CDC7 gene is overexpressed in some tumors and transformed cell lines. *Gene* 1998; 211(1): 133-40.
18. Dally RD, Woods TA. CDC7 inhibitors. Google Patents; CA2900773A1. 2014.
19. Clarke LE, Fontaine TJ, Hennessy J, et al. CDC7 expression in melanomas, Spitz tumors and melanocytic nevi. *Journal of Cutaneous Pathology* 2009; 36(4): 433-8.
20. Tekkesin MS, Mutlu S, Olgac V. The role of RANK/RANKL/OPG signalling pathways in osteoclastogenesis in odontogenic keratocysts, radicular cysts, and ameloblastomas. *Head Neck Pathol* 2011; 5(3): 248-53.
21. Kulkarni AA, Kingsbury SR, Tudzarova S, et al. CDC7 kinase is a predictor of survival and a novel therapeutic target in epithelial ovarian carcinoma. *Clinical Cancer Research* 2009; 15(7): 417-25.
22. Shi N, Xie W-B, Chen S-Y. Cell division cycle 7 is a novel regulator of transforming growth factor- β -induced smooth muscle cell differentiation. *Journal of Biological Chemistry* 2012; 287(9): 6860-7.
23. Seyedmajidi M, Shafaei S, Siadati S, et al. Immunohistochemical analysis of COX-2 expression in dentigerous cyst, keratocystic odontogenic tumor and ameloblastoma: A comparative study. *Dent Res J (Isfahan)* 2015 May-Jun; 12(3): 278-84.
24. Gurgel CAS, Ramos EAG, Azevedo RA, Sarmiento VA, da Silva Carvalho AM, dos Santos JN. Expression of Ki-67, p53 and p63 proteins in keratocyst odontogenic tumours: an immunohistochemical study. *Journal of Molecular Histology* 2008; 39(3): 311-6.
25. Sainsbury R, Proctor I, Rodriguez S, et al. Targeting DNA replication before it starts: Cdc7 as a therapeutic target in p53 mutant Her2 and triple negative breast cancer. *Breast Cancer Research* 2010; 12: 50.
26. Güler N, Çomunoğlu N, Cabbar F. Ki-67 and MCM-2 in Dental Follicle and Odontogenic Cysts: The Effects of Inflammation on Proliferative Markers. *The Scientific World Journal* 2012; 2012: 946060.

Modulation of Rat Liver Regeneration after Partial Hepatectomy by Dietary Cholesterol

Pavel Živný¹, Helena Živná^{2*}, Vladimír Palička¹, Lenka Žaloudková¹, Petra Mocková¹, Jolana Cermanová³, Stanislav Mičuda³

ABSTRACT

Introduction: The aim of study was to evaluate impact of long-term dietary cholesterol overload on the cholesterol homeostasis and liver regeneration.

Material and Methods: Serum lipid parameters, ¹⁴C-cholesterol incorporation, liver DNA synthesis and protein expression was determined in partially hepatectomized (PH) rats fed with a standard (SLD) or hypercholesterolemic (CHOL) diet.

Results: 29-day intake of CHOL diet before PH produced increase in serum total cholesterol, LDL lipoprotein, and triglyceride concentration. PH provoked decrease in serum total cholesterol and triglyceride concentration in both groups. PH was associated with increase in serum ALT activity more pronounced in CHOL animals. Hepatic DNA synthesis was increased after PH in both groups, but lower in CHOL. Hypercholesterolemic diet reduced the absorption of radiolabelled cholesterol in intestine and then activity in blood and liver. The ¹⁴C-cholesterol hepatic activities tend to increase after PH in both groups. CHOL diet produced up-regulation of Acyl-CoA:cholesterol acyltransferase-2 protein expression. PH was associated with increase of LDL receptor and Acyl-CoA:cholesterol acyltransferase-2 protein expression in both dietary groups.

Discussion: Liver regeneration after PH is negatively influenced by CHOL diet. The increased uptake of cholesterol in the liver after PH associated with up-regulation of LDL receptor protein expression suggests preferential use of extrahepatic cholesterol by the liver.

KEYWORDS

liver; partial hepatectomy; cholesterol; LDL receptor; ACAT-2; rat

AUTHOR AFFILIATIONS

¹ Institute of Clinical Biochemistry and Diagnostics, University Hospital, Charles University, Hradec Králové, Czech Republic

² Radioisotope Laboratories and Vivarium, Medical Faculty, Charles University, Hradec Králové, Czech Republic

³ Department of Pharmacology, Medical Faculty, Charles University, Hradec Králové, Czech Republic

* Corresponding author: Radioisotope Laboratories and Vivarium, Medical Faculty, Charles University, Šimkova 870, 500 38 Hradec Králové, Czech Republic; e-mail: zivna@lfhk.cuni.cz

Received: 10 January 2018

Accepted: 13 May 2018

Published online: 2 July 2018

Acta Medica (Hradec Králové) 2018; 61(1): 22–28

<https://doi.org/10.14712/18059694.2018.19>

© 2018 The Authors. This is an open-access article distributed under the terms of the Creative Commons Attribution License (<http://creativecommons.org/licenses/by/4.0>), which permits unrestricted use, distribution, and reproduction in any medium, provided the original author and source are credited.

INTRODUCTION

Hypercholesterolemia has been considered as a major risk factor for cardiovascular disease such as coronary heart disease and atherosclerosis (1), a leading cause of death and disability in developed countries. Moreover the role of cholesterol in the pathogenesis of non-alcoholic steatohepatitis (NASH) remains unclear. Results of Zhu et al. suggested that cholesterol markedly promoted apoptosis of steatotic HepG2 cells in vitro, likely through the up-regulation of Bax and caspase-3 expression. Other authors suggested that abnormal lipid metabolism may contribute to the increase of reactive oxygen species (ROS) and inflammation and induced NASH (2, 3).

Liver is the central organ in the regulation of whole-body cholesterol homeostasis. The role in the cholesterol metabolism is multiplex and includes the synthesis of cholesterol and cholesterol-carrying apoproteins; catabolism of cholesterol to bile acids; receptor-mediated clearance of cholesterol containing lipoproteins; and esterification of cholesterol (4, 5). Not surprisingly, high cholesterol dietary intake induces changes of these processes and invoke suppression of cholesterol *de novo* synthesis and increased storage of lipids in the liver (2, 6). In addition, long-term hypercholesterolemic diet is associated with potentiated signalling by adhesion molecules and activation of fat-storing cells to become fibrogenic effector leading to liver fibrosis (7, 8).

Partial hepatectomy (PH) in rats is widely used model to study liver regeneration, which is accompanied by cell division and by outstanding cell and organelle membrane production. This process requires quantity of cholesterol (9). Hepatocytes after PH proliferate synchronously, they enter in G1 phase and begin to synthesize DNA 18 h after PH and divide after 24 h. It has been shown that cholesterol is necessary in early G1 phase during cell duplication. During liver regeneration, an increase in chromatin cholesterol is observed between 6 and 18 h after hepatectomy (7). Therefore, appropriate cholesterol intake and balanced diet is essential for liver regeneration (9).

The aim of present study was (1) to evaluate impact of long-term dietary cholesterol overload on the cholesterol homeostasis and then (2) to evaluate the influence of this status on liver regeneration induced by surgical removal of 70% of liver parenchyma in rats. To obtain relevant information, changes in serum biochemical parameters, hepatic DNA synthesis, cholesterol content in the main organs of cholesterol turnover and hepatic expression of key enzymes of cholesterol metabolism were evaluated in these animals.

MATERIALS AND METHODS

PREPARATION OF LABORATORY DIET

Diet was prepared according to available literature (www.testdiet.com, www.dyets.com) from casein (PML Inc., Novy Bydzov, CZ), cornstarch (Skrobarny Pelhrimov, CZ), cellulose (Phrikolat, Chemische Erzeugnisse GmbH, Germany), choline chloride, L-cysteine, L-arginine and sucrose (Fisher Scientific, Ltd., Pardubice, CZ), corn oil

(CANO Ltd. Hermanuv Mestec, CZ), DL-methionine (Sigma-Aldrich, Ltd. Prague, CZ), mixture of vitamins and minerals according to AIN-93, TestDiet.

The half of the prepared diet was control diet (SLD). Second half of diet was enriched by cholesterol to the final concentration of 4% (CHOL). These diets were fabricated into pellets and dried in 60 °C in food dryer.

MATERIALS

Rabbit polyclonal anti-ACAT-2 (Acyl-coenzyme A: Cholesterol Acyltransferase-2, Cat. No. 100027) antibody and anti-LDL receptor (Cat. No. 10007665) polyclonal antibody was obtained from Cayman Chemical (Ann Arbor, MI, USA). Anti-HMG-CoA Reductase antibody was purchased from Chemicon (Billerica, MA, USA). Horseradish peroxidase-linked donkey anti-rabbit immunoglobulin G was purchased from GE Healthcare (Prague, CZ). All other reagents and supplies were obtained from Sigma Chemical Co. (St. Luis, MO) and SERVA Electrophoresis GmbH (Heidelberg, Germany), respectively, and were of the highest purity available.

ANIMALS

The Ethical Expert Committee of Medical Faculty, Charles University, Hradec Králové approved the experiment protocol (No. 20287/2005-30/300). All operations were performed in total ether anesthesia. Male Wistar rats (Biotest Inc., Konarovice, Czech Republic) were placed in plastic cages under standard conditions. They were in standard room temperature 22 ± 2 °C, twelve hours light/dark system, air humidity 30–70%. The rats (8 weeks old) were randomly divided into 2 groups, 24 rats each with starting body weight 256 ± 15 g. They were fed with above mentioned diets and drank tap water *ad libitum* for 29 days. 1st group: (SLD), were fed with standard laboratory diet, and 2nd group: (CHOL), were fed with cholesterol enriched diet (80–100 mg of cholesterol/rat/day). Eight rats from each group were sacrificed on 29th day of experiment (SLD-int, CHOL-int), others (8 + 8) underwent at the day 28 two third partial hepatectomy (PH) and then were sacrificed 18 hours (8 + 8 rats, SLD-18, CHOL-18), and 24 hours (8 + 8 rats, SLD-24, CHOL-24) after partial hepatectomy (10).

¹⁴C-cholesterol (37 kBq/100 g of body weight, APCzech, Prague, CZ) was administered p.o. 24 hours before sacrifice to intact rats or immediately after PH. The 3H-thymidin (740 kBq/100 g of body weight, Lacomel Ltd., Řež u Prahy, CZ) was administered i.v. 1 hour before sacrifice by exsanguination from abdominal aorta in all rats.

The liver was removed and immediately frozen in liquid nitrogen and stored at -80 °C until analyses.

ANALYSES

Serum total cholesterol, triglyceride (TAG) concentration and ALT activity (μ kat/l) was measured by automated enzymatic methods on Modular Roche analyser (Roche, Mannheim, Germany). Liver cholesterol concentration was determined using colorimetric kits (Lachema, Brno, CZ).

The activity of ^{14}C -cholesterol (Bq/g of tissue or ml of blood) was determined after ethanol-acetone extraction and saponification and radioactivity was quantitated by scintillation counting (11). Newly synthesized bile acids with incorporated ^{14}C -cholesterol in liver were assessed after ethanol extraction, precipitation by digitonin (10) and radioactivity was quantitated by scintillation counting. Liver DNA synthesis was determined by incorporation of methyl ^3H -thymidine to liver DNA (11). The radioactivity of the samples was measured by liquid scintillation system on Beckman Coulter LS 6000LL (Fullerton, CA, USA). The liver DNA content was determined with diphenylamine reagent (12).

WESTERN BLOT

Hepatic expression of key enzymes of cholesterol metabolism, namely 3-hydroxy-3-methylglutaryl coenzyme A (HMG-CoA) reductase, low-density lipoprotein (LDL) receptor, and acyl-coenzyme A:cholesterol acyltransferase (ACAT-2) was assessed by Western blot.

Membrane preparation. Samples were prepared as described previously (13). Briefly, livers were minced in ice-cold Tris-sucrose buffer containing 0.5 $\mu\text{g}/\text{mL}$ leupeptin, 0.5 $\mu\text{g}/\text{mL}$ pepstatin, 2 $\mu\text{g}/\text{mL}$ aprotinin, 50 $\mu\text{g}/\text{mL}$ benzamide, and 40 $\mu\text{g}/\text{mL}$ phenylmethylsulfonyl fluoride (PMSF) and homogenized. A membrane-enriched microsomal pellet was obtained from the postnuclear supernatant after a 100,000 g ultracentrifugation at 4 °C for 60 minutes. Acquired pellet was resuspended in Tris-HCl buffer. The protein concentration was determined with the BCA assay (Pierce, Rockford, IL, USA) and samples were stored at -80 °C.

Immunoblot analysis. Crude membrane-containing homogenates (50 μg) from freshly harvested livers were incubated with sample buffer at room temperature for 30 minutes and separated on a 7.5% polyacrylamide gel. After the proteins were transferred to a nitrocellulose membrane (Bio-Rad, Hercules, CA, USA), it was blocked for 1 h at room temperature with 5% nonfat dry milk in Tris-buffered saline containing 0.05% Tween 20 (TTBS). The membrane was then incubated with primary antibodies (1:500) for 1 h, washed, and incubated for 1 h with a peroxidase-conjugated secondary antibody (1:1,000). After washing five times with TTBS, the membranes were developed using enhanced chemiluminescent reagent (GE Healthcare, Prague, CZ) and subjected to autoluminography for 1–5 min. The immunoreactive bands on the exposed films were scanned with densitometer ScanMaker i900 (UMAX, Prague, CZ) and semiquantified using the QuantityOne imaging software (Bio-Rad).

HISTOLOGY

Liver tissue for histopathological examination was obtained from one standard site (*processus anterior dexter et processus caudatus lobi caudati*) and fixed in 10% buffered formalin. The 3 μm paraffin sections were stained with hematoxylin-eosin. Steatosis was graded by semi-quantitative analysis as follows: mild = 5–29%; moderate = 30–59%; and severe = more than 60% of hepatocytes affected. Each

biopsy was analyzed and graded by the same pathologist who was blinded to the rats group.

STATISTICS

Statistical analyses were performed by software SigmaStat 3.1 (Jandel Scientific®, San Rafael, CA, USA). Results are expressed as mean \pm SEM. Test used were *t*-test and ANOVA. One sign represents statistical significance $p < 0.05$, two signs are $p < 0.01$ and three signs represent $p < 0.001$, NS means “not significant”.

RESULTS

The results of serum biochemical analyses are summarized in Table 1. 29-day continual intake of high cholesterol diet in rats before PH produced 35% and 136% increase in serum total cholesterol and triglyceride. PH induced insignificant decrease in serum total cholesterol and triglyceride concentration in both SLD and CHOL groups. Alanine aminotransferase activities were significantly higher after PH in both dietary groups in comparison with intact rats, but changes were more pronounced in CHOL group.

Liver regenerative mechanism as evaluated by DNA synthesis and total content of DNA together with cholesterol content in the liver and changes in liver weights are listed in Table 2. PH in control diet fed animals produced increase in DNA synthesis in both SLD-PH groups with progression according to duration of PH. Total hepatic content of DNA and cholesterol was not changed in SLD-PH animals when compared with SLD-int. The rats of CHOL-int group had similar synthesis of DNA as SLD-int group. Nevertheless, PH in these animals produced significantly lower liver DNA synthesis 18 and 24 hours after surgical procedure together with decreased total content of liver DNA 24 hour after PH in comparison with respective SLD-PH rats. The liver weight in CHOL-int rats was significantly higher than in SLD-int, but smaller when compared with respective 24 hour PH groups. Liver cholesterol content was significantly higher in all CHOL rats comparing to corresponding SLD group. In comparison to respective intact groups, hepatic cholesterol content in both diet groups slightly decreased during 18 hour after PH.

To evaluate actual turnover of cholesterol in blood, liver and intestine, ^{14}C cholesterol was applied p.o. to all rats 18 or 24 hour before being sacrificed. The results of incorporation of radiolabeled cholesterol in tissues are presented in Table 3. While PH in SLD animals did not influenced the activities of cholesterol in intestine, or blood, the CHOL-int animals exerted significantly lower ^{14}C -cholesterol activities in all three evaluated compartments when compared with SLD-int group. The ^{14}C -cholesterol hepatic activities tend to increase after PH in both diet groups when compared with corresponding intact group.

To study expression of crucial receptors and enzymes involved in hepatic turnover of cholesterol we performed western blot analysis of HMG-CoA reductase, LDL receptor, and ACAT-2. Results are presented in Fig. 1–3. The HMG-CoA reductase protein expression was similar in intact animals of both diet groups. In addition, correspond-

Tab. 1 Serum concentrations of total cholesterol, triglycerides (mmol/l) and alanine-aminotransferase activities ($\mu\text{kat/l}$).

	SLD			CHOL		
	SLD-int	SLD-18	SLD-24	CHOL-int	CHOL-18	CHOL-24
Cholesterol	2.3 \pm 0.3	1.4 \pm 0.1 [†]	1.0 \pm 0.1 ^{††}	3.1 \pm 0.2 ^{**}	1.9 \pm 0.1 ^{††}	1.3 \pm 0.13 ^{††}
TAG	1.4 \pm 0.2	0.3 \pm 0.02 [†]	0.4 \pm 0.04 [†]	3.3 \pm 0.4 ^{***}	0.8 \pm 0.5 [†]	0.4 \pm 0.04 ^{††}
ALT	0.7 \pm 0.09	6.8 \pm 1.0 ^{***}	6.2 \pm 1.8 ^{**}	0.7 \pm 0.07	20.9 \pm 10.7 ^{††***†}	9.5 \pm 1.8 ^{***}

Values are means \pm SEM (n = 8).

* P < 0.05, ** P < 0.01, *** P < 0.001 all groups vs. SLD-intact animals;

† P < 0.05, †† P < 0.001 PH group vs. corresponding intact group (SLD or CHOL);

† P < 0.05 respective CHOL-PH group vs. corresponding SLD-PH group

Tab. 2 Specific activity (s.a. – synthesis) of liver DNA (Bq/ μg DNA), total content (t.c.) of liver DNA ($\mu\text{g} \times 10^3/\text{g}$ liver), weight of liver remnant (g/100 g of body weight) and liver cholesterol concentration ($\mu\text{g/g}$).

	SLD			CHOL		
	SLD-int	SLD-18	SLD-24	CHOL-int	CHOL-18	CHOL-24
s.a. DNA	0.2 \pm 0.03	2.3 \pm 0.44 [†]	11.2 \pm 1.1 ^{††}	0.3 \pm 0.02	1.1 \pm 0.26 ^{††}	6.1 \pm 0.8 ^{†††}
t.c. DNA	1.7 \pm 0.04	1.9 \pm 0.1	2.0 \pm 0.1	1.5 \pm 0.1	1.8 \pm 0.1	1.8 \pm 0.1 ^{††}
Liver weight	3.5 \pm 0.2	1.4 \pm 0.1	2.1 \pm 0.1	5.3 \pm 0.3 ^{***}	1.8 \pm 0.1 ^{††}	1.8 \pm 0.1 ^{††}
Liver cholesterol	4.3 \pm 0.2	3.9 \pm 0.2	4.8 \pm 0.3	12.8 \pm 0.8 ^{***}	10.9 \pm 0.6	12.2 \pm 0.6

Values are means \pm SEM (n = 8).

* P < 0.05, ** P < 0.01, *** P < 0.001 all groups vs. SLD-intact animals;

† P < 0.05, †† P < 0.001 PH group vs. corresponding intact group (SLD or CHOL);

† P < 0.05 respective CHOL-PH group vs. corresponding SLD-PH group;

xxx P < 0.001 SLD-18 vs. SLD-24 and CHOL-18 vs. CHOL-24

Tab. 3 ¹⁴C-cholesterol activities in selected tissues, in blood and as bile acid in liver tissue (Bq/g of tissue, Bq/ml of blood).

	SLD			CHOL		
	SLD-int	SLD-18	SLD-24	CHOL-int	CHOL-18	CHOL-24
Intestine	1952 \pm 797	1948 \pm 473	2941 \pm 769	335 \pm 64 [*]	1074 \pm 277	845 \pm 219
Blood	616 \pm 44	322 \pm 70	720 \pm 66	312 \pm 71 [*]	312 \pm 41	427 \pm 73
Liver	833 \pm 123	1467 \pm 235	1895 \pm 402	228 \pm 36 [*]	1082 \pm 159	845 \pm 162
Bile acid in liver tissue	71.2 \pm 15.1	74.3 \pm 10.9	84.9 \pm 17.4	52.1 \pm 14.3	55.9 \pm 10.8	54.7 \pm 12.4

Values are means \pm SEM (n = 8).

* P < 0.05, ** P < 0.01, *** P < 0.001 all groups vs. SLD-intact animals

ing progression of changes was detected in all groups after PH. We observed insignificant decrease of HMG-CoA reductase 18 hours after PH and then increase 24 hours after PH (Fig. 1).

The expression of ACAT-2 was slightly induced in intact cholesterol fed rats (Fig. 2). The SLD rats had significantly elevated ACAT-2 expression especially 18 hour after PH in comparison with SLD intact rats. Similarly, the rats of CHOL group had significant elevation of ACAT-2 expression after both intervals of PH.

The rats in CHOL group had insignificantly lower LDL receptor protein expression before PH versus SLD rats (Fig. 3). The significant increase in LDL receptor protein expression was observed in both dietary groups 18 hours and 24 hours after PH with changes being more intensive in CHOL rats.

Macroscopic and microscopic examination of the liver of SLD and CHOL animal is presented in Fig. 4–7.

Liver of a rat fed by SLD diet shows normal macroscopic finding (Fig. 4).

The liver tissue of a control rat shows no histopathologic changes (Fig. 5).

The liver of a CHOL rat shows macroscopic steatosis (Fig. 6).

The liver after a 29 days CHOL diet shows lobular microvesicular steatosis (>30%), no inflammatory cells were observed (Fig. 7).

DISCUSSION

In the present study, we demonstrated significant changes in cholesterol homeostasis after long-term hypercholesterolemic diet in rats which were associated with impaired liver regeneration. High cholesterol intake induced increased serum total cholesterol and TAG concentrations.

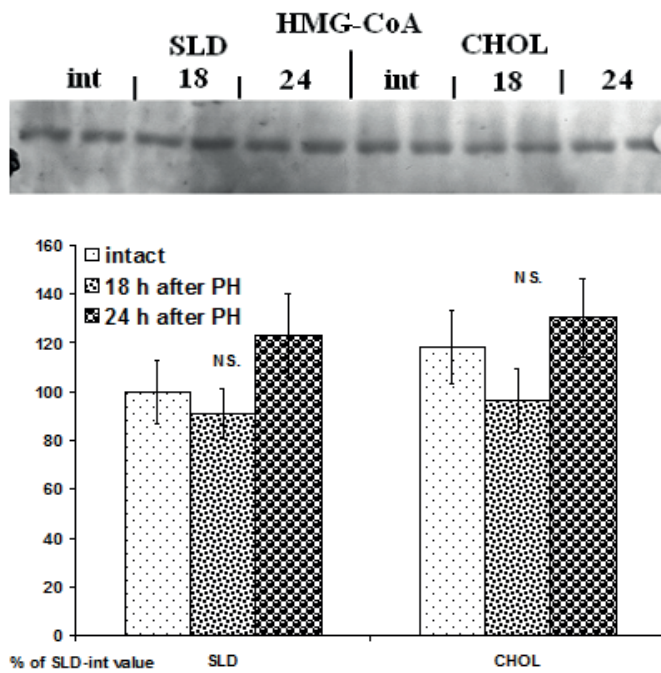


Fig. 1 Representative Western blot and group data depicting HMG-CoA reductase protein expression in the liver of control (SLD – standard laboratory diet) and cholesterol overloaded (CHOL) rats before (intact) and 18 or 24 hour after PH. Data are means \pm SEM ($n = 8$ in each group). All data were compared with SLD-intact (rats on standard chow before PH). NS, not significant.

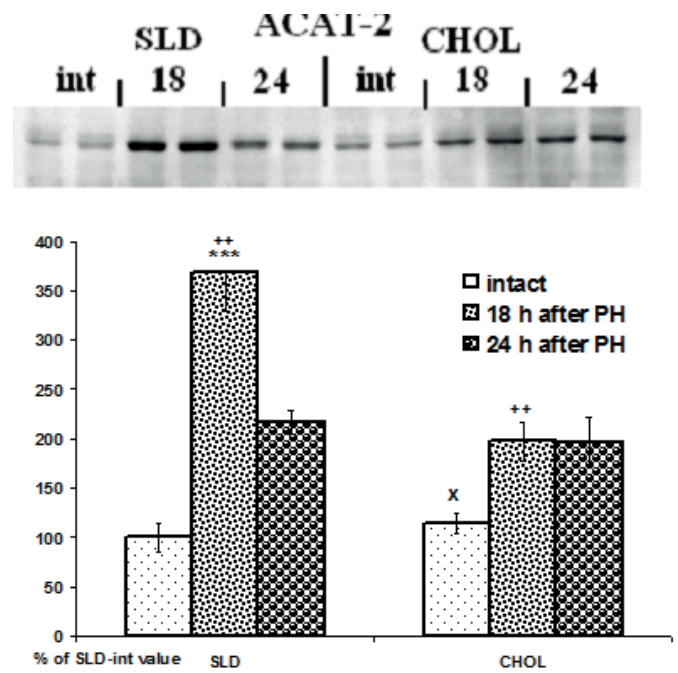


Fig. 2 Representative Western blot and group data depicting Acyl-CoA:cholesterol acyltransferase (ACAT-2) protein expression in the liver of control (SLD – standard laboratory diet) and cholesterol overloaded (CHOL) rats before (intact) and 18 or 24 hour after PH. Data are means \pm SEM ($n = 8$ in each group). Data were compared with SLD-intact (rats on standard chow before PH). Statistical significance *** vs. SLD-int, ++ SLD-18 vs. CHOL-18, x vs. SLD-int.

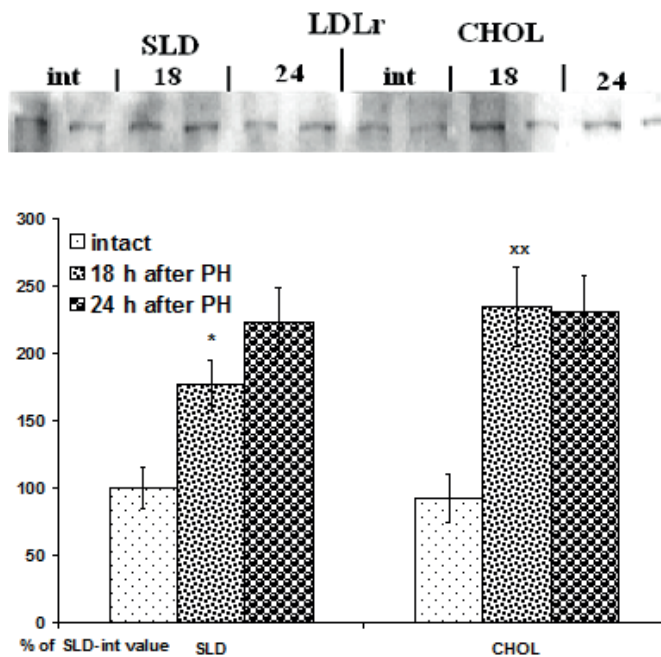


Fig. 3 Representative Western blot and group data depicting LDL receptor protein expression in the liver of control (SLD – standard laboratory diet) and cholesterol overloaded (CHOL) rats before (intact) and 18 or 24 hour after PH. Data are means \pm SEM ($n = 8$ in each group). All data were compared with SLD-intact (rats on standard chow before partial hepatectomy). Statistical significance * vs. SLD-int, xx vs. CHOL-int.

CHOL rats developed steatosis, which was proven macroscopically and microscopically. PH in these animals lead to lower hepatic DNA synthesis, DNA content and cholesterol uptake and increased ALT activity in comparison to intact animals which indicate problems in liver reparative processes. In addition, we observed induction of LDL receptor protein expression and increased uptake of cholesterol by the liver after PH.

The high-cholesterol diet consumption reduced cholesterol absorption from intestine in mice (14), in rats (15), and probably in humans (16). The assumed mechanism is decrease of intestinal cholesterol absorption by up-regulation of adenosine triphosphate-binding cassette cholesterol transporter – Abcg5, Abcg8 (15) or a Niemann-Pick C1 Like 1 (NPC1L1) protein localized in jejunal enterocytes, which are critical for intestinal cholesterol absorption (17). These data comply with the results of our study where we demonstrated that the rats of CHOL group had inhibited exogenous cholesterol absorption, and ^{14}C -cholesterol was increased in faeces in comparison with SLD group (unpublished observation). This fact is agreed by significant decrease of ^{14}C cholesterol activities in intestinal wall tissues in CHOL groups (and consequently in blood, liver and intrahepatic bile acid).

We observed slight increase in hepatic ACAT-2, and unchanged LDL-receptor and HMG-CoA reductase protein expression between SLD and CHOL rats before PH. Spectrum of studies dealing with these protein expressions after hypercholesterolemic diet brought controversial results. Our results are in agreement with some of these reports pointing to induction of ACAT-2 and minimal

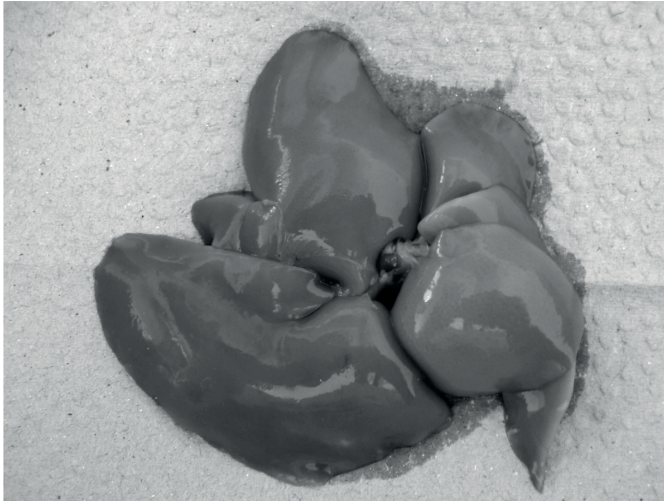


Fig. 4 Macroscopic view of liver from intact rat SLD group after exsanguination. Homogenous structure of intact liver.

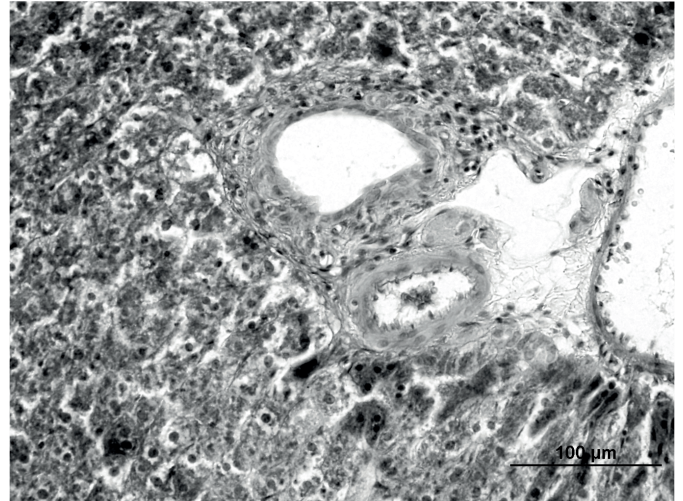


Fig. 5 Histology of liver tissue from intact rat SLD group. Normal liver shows regular lobular architecture (HE, magnification 200×).

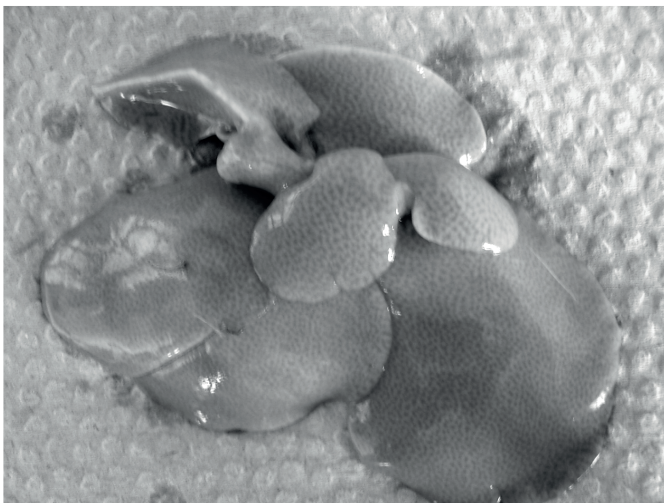


Fig. 6 Macroscopic view of liver from intact rat CHOL group after exsanguination. Pale steatotic liver.

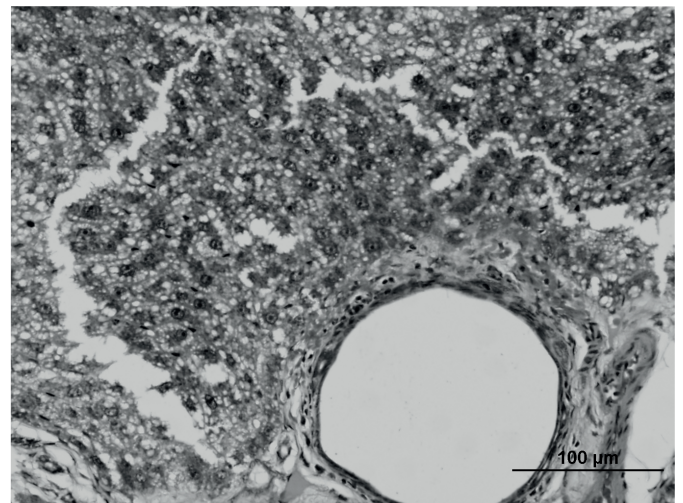


Fig. 7 Histology of liver from intact rat CHOL group. The liver after a 29 days CHOL diet show lobular microvesicular steatosis (>30%) and no inflammatory cells were observed (HE, artificial laceration (magnification 200×).

changes of HMG-CoA reductase and LDL receptor during long-term cholesterol overload (5, 6, 18). One explanation for minimal changes in respective hepatic proteins observed in our study might be the decreased intestinal absorption of cholesterol, which reduces influence of dietary cholesterol on the liver proteins.

Liver regeneration after PH is accompanied by cell division and (cell and organelle) membrane production is a process requiring cholesterol (7). The rats after PH lost about 67–70% of liver parenchyma together with cholesterol synthesis enzymes and cholesterol store, nevertheless they have to induce regenerative processes. As a consequence, serum cholesterol concentration decreased after PH in both groups, which comply with our previous results (19). Similarly in humans, hypocholesterolaemia is a frequent and typical phenomenon of many acute situations in the critically ill (20). Albi et al. (9) proved that hepatic cholesterol increases during liver regeneration after PH, first as a linked fraction and then, when DNA synthe-

sis starts, as a free fraction. Herein, we demonstrated that regenerating liver tissue in rats after PH gained preferentially cholesterol from circulation. This concept is supported by:

1. Increased content of ^{14}C -cholesterol in the liver after PH indicating increased uptake from blood. This effect is most probably consequence of observed up-regulation of liver LDL receptor expression after PH. It suggests the effort of remnant hepatocytes to use LDL cholesterol, mainly in rats of CHOL groups which is in accordance with the results of other authors (21, 22). In agreement, Bocchetta et al. (23) demonstrated an induction of LDL receptor gene expression shortly (2–4 h) after PH.
2. Up-regulation of liver ACAT-2 synthesis for esterification of (newly) absorbed liver cholesterol. Our results show, that ACAT-2 expression increased significantly in all PH groups indicating activation of regenerative processes such membrane component synthesis.

3. Stable expression of HMG-CoA reductase after PH, with only an insignificant decrease 18 hour after PH and slight increase 24 hours after PH. Similarly, Cheng et al. (24) demonstrated that cholesterol synthesis was selectively decreased 24 hours after PH in rat hepatocytes. Bakalar et al. (25) proved decrease of cholesterol precursor synthesis as a major cause of hypocholesterolemia in the critically ill patients with multiple trauma.

We evaluated DNA synthesis as the marker of liver regeneration. After PH in SLD animals we observed steady increase in ³H-thymidin incorporation indicating liver regeneration. This process was markedly delayed in CHOL group. We suppose that physiological turnover of adequate endogenous and exogenous cholesterol makes better conditions for triglyceride metabolism with early onset and advantageous course of liver regeneration. Blaha et al. (26) showed necessity of lipids for liver regeneration after PH which was significantly better in balanced enteral feeding in comparison with overfeeding. The rats fed by high cholesterol diet had blocked the cholesterol absorption from intestine, and endogenous synthesis of cholesterol is not flexible enough (24, 25), which might be followed by deceleration of DNA liver synthesis.

The negative effect of high cholesterol diet demonstrated by the course of liver regeneration was expressed among others also by higher transaminase activities in CHOL groups (especially 18 hours after PH). The reason of this fact is not completely resolved. It may be problem originating from higher membrane fluidity (8), severe steatosis (2), or impaired ACAT-2-mediated protection of hepatocytes against free cholesterol toxicity (27).

High cholesterol diet consumption in CHOL group leads to status with higher stores of cholesterol in the liver. The rats of CHOL group had liver steatosis, in spite of that both diets (SLD and CHOL) had an identical content of non-steroid lipids (5% oil of corn). Therefore, the liver steatosis was the result of abundant intake of exogenous cholesterol only, and subsequent different triglyceride distribution. This is in agreement with previously reported rapid deposition of lipid droplets in the liver during a high cholesterol diet (2). The lipid accumulation in the liver results from an imbalance between hepatic fatty acid inflow, triglyceride synthesis and excretion (3).

In conclusion, the liver regeneration in rats after PH is negatively influenced by high cholesterol diet. PH produced preferential use of extrahepatic cholesterol by the liver through LDL receptor up-regulation. However, the uptake of cholesterol to liver was less effective in CHOL rats after PH following delayed liver regeneration.

ACKNOWLEDGEMENTS

Supported by projects: UHHK, 00179906 and SVV 260689.

The authors thank Jitka Hajková, Lenka Kriesfalusyová and Dagmar Ježková for excellent technical assistance and Iva Zadrobilková and Naďa Horaková for diet preparation.

REFERENCES

- Seman LJ, DeLuca C, Jenner JL, et al. Lipoprotein(a)-cholesterol and coronary heart disease in the Framingham Heart Study. *Clin Chem* 1999; 45: 1039–46.
- Zhu C, Xie P, Zhao F, Zhang L, An W, Zhan Y. Mechanism of the promotion of steatotic HepG2 cell apoptosis by cholesterol. *Int J Clin Exp Pathol* 2014; 15: 6807–13.
- Mao J, Liu W, Wang Y. Apolipoprotein A-I expression suppresses COX-2 expression by reducing reactive oxygen species in hepatocytes. *Biochem Biophys Res Commun* 2014; 454: 359–63.
- Liang K, Vaziri ND. HMG-CoA reductase, cholesterol 7 α -hydroxylase, LCAT, ACAT, LDL receptor, and SRB-1 in hereditary analbuminemia. *Kidney Int* 2003; 64: 192–8.
- Lee JY, Carr TP. Dietary Fatty Acids Regulate Acyl-CoA:Cholesterol Acyltransferase and Cytosolic Cholesteryl Ester Hydrolase in Hamsters. *The American Society for Nutritional Sciences J Nutr* 2004; 134: 3239–44.
- Ness GC, Gertz KR. Hepatic HMG-CoA reductase expression and resistance to dietary cholesterol. *Exp Biol Med (Maywood)* 2004; 229: 412–6.
- Albi E, Magni MV. The presence and the role of chromatin cholesterol in rat liver regeneration. *J Hepatol* 2002; 36: 395–400.
- Qin C, Nagao T, Grosheva I, et al. Elevated plasma membrane cholesterol content alters macrophage signaling and function. *Arterioscler Tromb Vasc Biol* 2006; 26: 372–8.
- Albi E, Viola Magni MP. The role of intranuclear lipids. *Biol Cell* 2004; 96: 657–67.
- Sehayek E, Ono JG, Shefer S, et al. Biliary cholesterol excretion: a novel mechanism that regulates dietary cholesterol absorption. *Proc Natl Acad Sci USA* 1998; 95: 10194–9.
- Short J, Zemel R, Kanta J, Lieberman I. Stimulation of deoxyribonucleic acid synthesis in the liver parenchymal cells of the intact rats. *Nature* 1969; 223: 956–57.
- Burton K. A study of the condition and mechanism of the colorimetric estimation of deoxyribonucleic acid. *Biochem J* 1956; 62: 315–23.
- Micuda S, Fuksa L, Brcakova E, et al. Zonation of Mrp2 in rat liver during induction. *Journal of Gastroenterology and Hepatology. J Gastroen Hepatol* 2008; 23(7 Pt 2): e225–30.
- Duan LP, Wang HH, Wang DQ. Cholesterol absorption is mainly regulated by the jejunal and ileal ATP-binding cassette sterol efflux transporters Abcg5 and Abcg8 in mice. *J Lipid Res* 2004; 45: 1312–23.
- Kamisako T, Ogawa H. Effect of bile duct obstruction on the expression of intestinal mRNA related to cholesterol and bile acid metabolism in the rat. *J Gastroenterol Hepatol* 2007; 22: 125–31.
- Klett EL, Lee MH, Adams DB, et al. Localization of ABCG5 and ABCG8 proteins in human liver, gall bladder and intestine. *BMC Gastroenterol* 2004; 214: 21.
- Davis HR, Zhu LJ, Hoos LM, et al. Niemann-Pick C1 Like 1 (NPC1L1) is the intestinal phytosterol and cholesterol transporter and a key modulator of whole-body cholesterol homeostasis. *J Biol Chem* 2004; 279: 33586–92.
- Rudel LL, Davis M, Sawyer J, et al. Primates highly responsive to dietary cholesterol up-regulate hepatic ACAT2, and less responsive primates do not. *J Biol Chem* 2002; 277: 31401–6.
- Zivna H, Zivny P, Palicka V, Simakova E. Influence of High Cholesterol Diet and Pravastatin Sodium on the Initiation of Liver Regeneration in Rats after Partial Hepatectomy. *Nutrition* 2002; 18: 51–5.
- Manka P, Olliges V, Bechmann LP, et al. Low levels of blood lipids are associated with etiology and lethal outcome in acute liver failure. *PLoS One* 2014; 9: e102351.
- Fushimi T, Suruga K, Oshima Y, et al. Dietary acetic acid reduces serum cholesterol and triacylglycerols in rats fed a cholesterol-rich diet. *Br J Nutr* 2006; 95: 916–24.
- Hoekstra M, Out R, Kruijt JK, et al. Diet induced regulation of genes involved in cholesterol metabolism in rat liver parenchymal and Kupffer cells. *J Hepatol* 2005; 42: 400–7.
- Bocchetta M, Bruscalupi G, Castellano F, et al. Early induction of LDL receptor gene during rat liver regeneration. *J Cell Physiol* 1993; 156: 601–9.
- Cheng HC, Yang CM, Shiao MS. Zonation of cholesterol and glycerolipid synthesis in regenerating rat livers. *Hepatology* 1993; 17: 280–6.
- Bakalar B, Hyspler R, Pachel J, Zadac Z. Changes in cholesterol and its precursors during the first days after major trauma. *Wien Klin Wochenschr* 2003; 115: 775–9.
- Blaha V, Cervinkova Z, Simek J, et al. Long- and medium-chain triacylglycerols in nutritional support of liver regeneration of partially hepatectomized rats. *Physiol Res* 1999; 48: 457–63.
- Chang CC, Sakashita N, Ornvold K, et al. Immunological quantitation and localization of ACAT-1 and ACAT-2 in human liver and small intestine. *J Biol Chem* 2000; 275: 28083–92.

Giant Uterine Leiomyoma in a Young Woman as an Incidental Finding After a Car Accident: a Case Report

Vladimír Bartoš^{1,*}, Peter Korec², Robert Ficek³

ABSTRACT

Leiomyomas are the most common benign tumor of the uterus. Occasionally, they may reach an extreme dimension. The authors present a case of a 44-year old woman, who suffered a car accident as a driver of personal motor vehicle. At the hospital, a huge tumor mass filling the entire abdominopelvic cavity was incidentally detected. The patient admitted a progressive abdominal enlargement for the last 5 years. An urgent laparotomy was performed, during which a giant, well-demarcated tumor arising from the uterine body had been disclosed. It was completely surgically removed and sent for histopathology. Grossly, the tumor measured 30 × 30 × 20 cm in the largest diameters and weighed 8.1 kg. The tissue was markedly edematous with foci of massive hemorrhages and contained confluent pseudocystic formations of various sizes, filled with a fluid and fresh blood. Solid foci of rubber consistency were also visible. Microscopic examination revealed a conventional subserous uterine leiomyoma with marked regressive and degenerative changes. Giant uterine leiomyomas occur extremely rare, but because of the often unexpected finding and atypical presentation, they may represent a great diagnostic challenge for both, pathologists and clinicians. At the biopsy examination, a multiple-section sampling is very important to avoid the possibility of underlying malignancy.

KEYWORDS

uterine leiomyoma; giant size; degenerative changes

AUTHOR AFFILIATIONS

¹ Department of Pathology, Faculty Hospital in Žilina, Slovakia

² Department of Surgery, Faculty Hospital in Žilina, Slovakia

³ Department of Gynecology and Obstetrics, Faculty Hospital in Žilina, Slovakia

* Corresponding author: Björnsonova 3/5, Martin, 036 01, Slovakia; e-mail: vladim.bartos@gmail.com

Received: 7 August 2017

Accepted: 12 February 2018

Published online: 2 July 2018

Acta Medica (Hradec Králové) 2018; 61(1): 29–32

<https://doi.org/10.14712/18059694.2018.20>

© 2018 The Authors. This is an open-access article distributed under the terms of the Creative Commons Attribution License (<http://creativecommons.org/licenses/by/4.0>), which permits unrestricted use, distribution, and reproduction in any medium, provided the original author and source are credited.

INTRODUCTION

Leiomyomas are the most common benign tumor of the uterus occurring in 30–50% of women between 30–50 years of age (1). In biopsy practice, they are found in up to 75% of hysterectomy specimens when they are systematically search for (2). Multiple lesions are present in two-thirds of the women with these neoplasms. The etiopathogenesis is still unclear but it seems that hormonal stimulation by estrogen and possibly progesterone plays a key role (2). Based on location they are classified as intramural (the most common form), submucosal and subserosal (2). The size of leiomyomas may vary from diminutive to huge tumors. They are often asymptomatic, but larger lesions produce a variety of clinical symptoms, such as dysmenorrhea, abnormal bleeding, pelvic discomfort or pain (2). On occasion, these tumors may reach an extreme size. The authors of the article present an unusual case of a giant uterine leiomyoma in a young woman that was incidentally diagnosed after a car accident.

CASE PRESENTATION

A 44-year old woman suffered a car accident in the city street as a driver of personal motor vehicle. She was immediately transported to the hospital by Emergency Rescue Service. During transport, the patient was conscious and communicated. A preliminary physical examination showed mild external injuries of the body (mainly contusions of the thorax and abdomen). At the hospital, urgent computed tomography (CT) scan revealed fractures of sternum and the right ribs, contusions of the right lungs and the liver and hemoperitoneum. However, as an incidental finding, a huge tumor mass filling the entire abdominopelvic cavity was detected. It was inhomogeneous, containing multicystic and solid components. Grossly, a woman had visibly enlarged abdomen. The patient admitted a progressive abdominal enlargement for the last 5 years, but she “had no time to visit the doctors”. An urgent laparotomy was performed, during which a giant, well-demarcated tumor arising from the uterine body had been disclosed (Figure 1). It grew expansively and compressed the intestines and visceral organs. No tumor implants on the omentum or visceral peritoneum were found. A gynecologist was called *ad hoc* into the operating room to consult the situation and further steps. The tumor was completely resected and sent for histopathology. Uterus and adnexa were retained *in situ*. As for traumatic injuries, surface laceration of the liver parenchyma was detected and sutured, as well as hemoperitoneum was evacuated. As the domain of our article is uterine neoplasm, in the next text, we focus on tumor aspects of the case. We only briefly mention, the car-accident related injuries did not have any serious consequences. Additionally it was found out, the patient was a nullipara, but she reported an abortion 15 years ago.

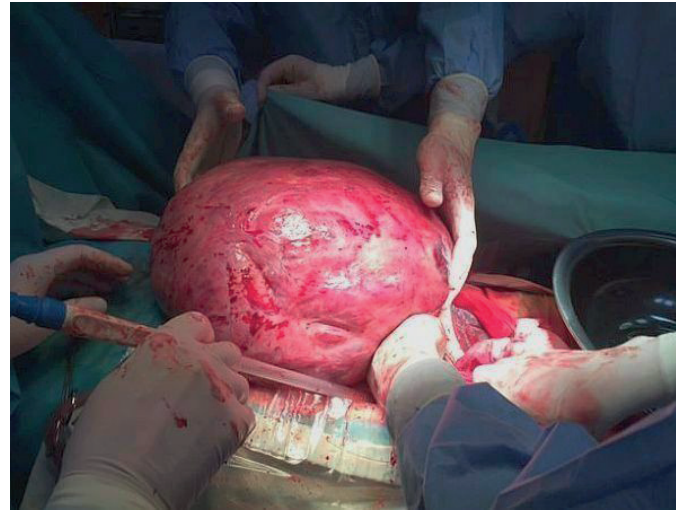


Fig. 1 Giant tumor mass revealed at laparotomy.

MATERIAL AND METHODS

Macroscopically, the tumor had an irregular shape, it measured 30 × 30 × 20 cm in the largest diameters and weighed 8.1 kg. On the surface, it was smooth and had a gray to gray-yellowish color with multiple small hemorrhages (Figure 2). Serial cut sections revealed very heterogeneous appearance, both of the structure and of the color (Figure 3). The tissue was markedly edematous with foci of massive hemorrhages and contained confluent pseudocystic formations of various sizes, filled with a fluid and fresh blood. Further, solid foci of rubber consistency and brown-yellowish color were also visible. Some of them were hard and calcified. Numerous tissue sections were taken, routinely processed in paraffin blocks (total of 45 blocks), stained with hematoxylin and eosin (H&E) and investigated in the light microscope. An immunohistochemical analysis was also performed.

RESULTS

Histopathologic examination identified a conventional subserous uterine leiomyoma with marked regressive changes, prominent edema with pseudocystic degeneration and multifocal fresh hemorrhages. No hemosiderin pigment was detected. Well-preserved tumor tissue was found particularly at the periphery of lesion. It consisted of dense interlacing fascicles of smooth muscle cells without a nuclear pleomorphism or increased mitotic count (Figure 4). Some solid tumor areas showed an extensive hyalinisation and dystrophic calcification. Immunohistochemically, the neoplastic cells were strongly positive for α -smooth muscle actin (clone 1A4, Dako), desmin (clone D33, Dako) (Figure 5) and h-caldesmon (clone h-CD, Dako). Proliferative activity (Ki-67, clone MM1, Leica) did not exceed 1%. No coagulative necroses were detected. There were not found any signs of malignancy. Five days after the first surgery, a laparotomy was repeated at the Depart-



Fig. 2 Tumor after surgical removal (post fixation in formalin).

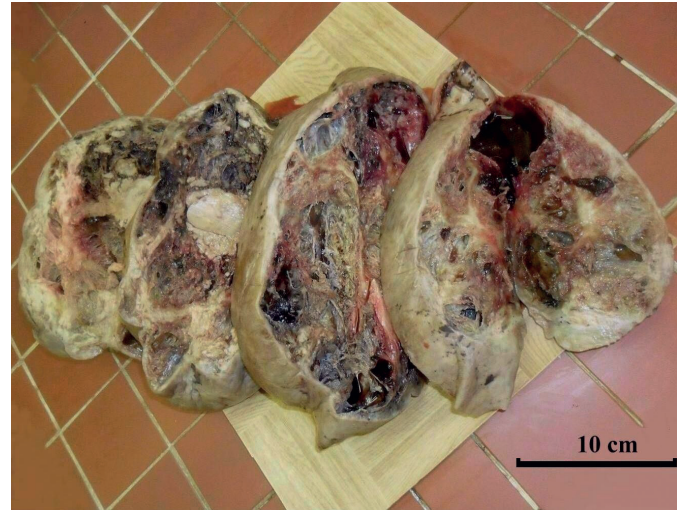


Fig. 3 Transversal sections through tumor (post fixation in formalin).

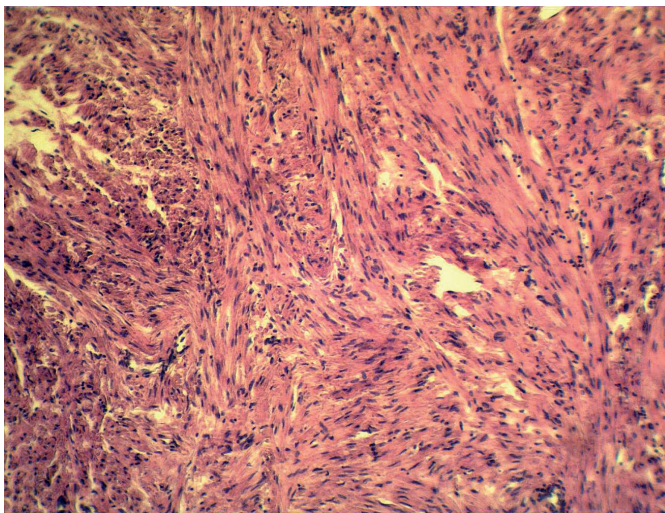


Fig. 4 Histomorphology of conventional leiomyoma (H&E, magnification 200 \times).

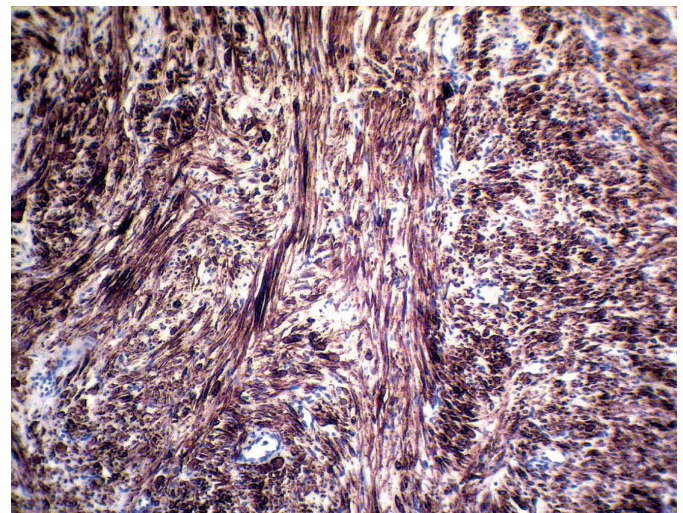


Fig. 5 Diffuse immunoreactivity of tumor for desmin (clone D33, magnification 200 \times).

ment of Gynecology, during which a resection of the uterine fundus containing a solitary intramural nodule (2.5 cm in the largest diameter) had been performed. Histologically, this nodular lesion was a conventional leiomyoma. The patient was discharged from the hospital on the 15th day after the first operation. Since she come from another district, at the time of writing this article we had not further informations about her.

DISCUSSION

Leiomyomas of the uterus belong to one of the most frequent diagnosis in a routine gynecologic and pathologic practice. These tumors may often reach large size, but such huge lesions as presented in our article are exceedingly rare. Although there is no consensual criterium for the definition of "giant" uterine leiomyoma, we reviewed the

recent papers publishing similar case reports using such terminology. They are briefly summarized in Table 1 (references 3-14). According to these literature sources (including our present case), the largest diameter of lesions ranged from 24.2 to 62 cm and a weight varied from 6.5 to 28.1 kg. They occurred in women between 33-63 years of age (mean 45 years). The most common clinical symptoms were abdominal distention, abnormal uterine bleeding, local pressure and pain. None of these cases was discovered as an incidental finding, which is a great peculiarity of our report. The potential for uterine leiomyomas to grow to an extreme size without significant clinical difficulties is quite notable. This is likely due to the relatively large volume of the abdominal cavity, the distensibility of the abdominal wall and the slow growth rate of these tumors. Especially subserosal lesions may be asymptomatic for a long time and thus, they sometimes become very large before the patient becomes aware of them.

Tab. 1 A summary of recent case reports describing giant uterine leiomyomas.

References	Age	Tumor size	Tumor weight
Moris et al. (2014)	39 years	62 × 39 × 21 cm	28.1 kg
Săvulescu et al. (2011)	45 years	33 × 28 × 22 cm	18.1 kg
Wroński (2014)	63 years	24.2 × 17.3 cm	not available
Funaki et al. (2013)	31 years	40 × 40 × 30 cm	8 kg
Kalayci et al. (2015)	49 years	33 × 25 cm	not available
Rahman et al. (2016)	46 years	43 × 32 × 23 cm	11.6 kg
Reshmy et al. (2015)	50 years	30 × 28 cm	not available
Ramteke et al. (2016)	40 years	26 × 23 × 18 cm	6.5 kg
Aydin et al. (2013)	58 years	33 × 20 × 18 cm	not available
Steward et al. (2011)	33 years	31 × 26 × 14 cm	11.6 kg
Müller & Břeský (2016)	42 years	> 30 cm	15.6 kg
Rajender Prasad et al. (2015)	45 years	33 × 28 × 22 cm	20 kg
present case	44 years	35 × 30 × 20 cm	8.1 kg

Larger uterine leiomyomas are frequently accompanied by prominent regressive and degenerative changes. Hyaline fibrosis and edema of tumor tissue are the most common one and are observed in up to 60% and 50% of all microscopically investigated leiomyomas of the uterus, respectively (2). Approximately 10% of them displays significant areas of hemorrhages (2). Pseudocystic degeneration occurs in about 4% of the cases (2) and it is usually extreme sequelae of edema. Dystrophic calcification may be found in 4% of all uterine leiomyomas (2), especially within fibrohyalinized regions. It is understandable, these changes become more prominent in huge tumors that have been growing for a long time. As a tumor progressively enlarges, it outgrows its blood supply, resulting in various types of degeneration. As a result they may create heterogeneous or unusual microscopic appearances that contribute to diagnostic confusion.

In conclusion, giant uterine leiomyomas occur extremely rare, but because of the often unexpected finding and atypical presentation, they may represent a great diagnostic challenge for both, pathologists and clinicians. At the biopsy examination, a multiple-section sampling is very important to avoid the possibility of underlying malignancy. A minimal sampling should include one tissue section per each 1 cm of tumor diameter. In our case, despite numerous tissue specimens investigated, no histologic features of malignancy were found.

ACKNOWLEDGEMENTS

The authors would like to thank all physicians from Faculty Hospital in Žilina, who participated on treatment and clinical management of the patient.

REFERENCES

1. Sklářová R. Klasifikace děložní myomatozy a její diagnostika ve vztahu k reprodukčním dysfunkcím. *Prakt Gyn* 2014; 18: 259–64.
2. Zaloudek C, Hendrickson MR. Mesenchymal Tumors of the Uterus. In: Kurman RJ (Ed). *Blaustein's Pathology of the Female Genital Tract*. 5th Edition, Springer Verlag, 2002: 564–78.
3. Moris D, Vernadakis S. Giant uterine leiomyoma mimicking pregnancy. *Mayo Clin Proc*, 2014; 89: e53–4.
4. Săvulescu F, Iordache I, Albița O, et al. Giant uterine leiomyoma. *Chirurgia (Bucur)* 2011; 106: 665–8.
5. Wroński K. Giant uterine leiomyoma – case report and review of literature. *New Medicine* 2014; 18: 89–91.
6. Funaki K, Fukunishi H, Tsuji Y, Maeda T, Takahashi T. Giant cystic leiomyoma of the uterus occupying the retroperitoneal space. *J Radiol Case Rep* 2013; 7: 35–40.
7. Kalayci TO, Akath AN, Sönmezgöz F, Şamdancı ET. A giant subserosal uterine leiomyoma mimicing and abdominal mass: multimodal imaging data. *Acta Medica Iranica* 2015; 53: 246–9.
8. Rahman H, Sharma BK, Khaldia E, Pathak R, Dubey S. Giant leiomyoma uterus with myomatous erythrocytosis syndrome: A rare case report. *J Cases Obstet Gynecol* 2016; 3: 88–91.
9. Reshmy JR, Bharti M, Rahul R. Giant cystic leiomyoma masquerading as ovarian tumour – case report. *Sch J Med Case Rep* 2015; 3: 608–10.
10. Ramteke S, Joshi P, Zararia A, Dharmale D. Fast growing giant intramural leiomyoma – a case report. *Int J Health Sci Res* 2016; 6: 542–5.
11. Aydin C, Eriş S, Yalçın Y, Sen Selim H. A giant cystic leiomyoma mimicking an ovarian malignancy. *Int J Surg Case Rep* 2013; 4: 1010–2.
12. Steward RG, Denhartog HW, Katz AR. Giant uterine leiomyomata. *Fertil Steril* 2011; 95: 1121.e15–7.
13. Müller R, Břeský P. Obrovský děložní myom – kazuistika. *Čes Gynek* 2016; 81: 71–5.
14. Rajender Prasad S, Nikhil S, Kumud S, Akanksha S, Atul J, Akshay P. Giant uterine leiomyoma and review of literature. *Int J Med Sci Clin Invent* 2015; 2: 640–4.

A Bilateral, Non-syndromic, Type III Second Branchial Arch Sinus in a Neonate: a Case Report

Ioannis Patoulas¹, Evangelia Rachmani¹, Konstantinos Farmakis¹, Vasileios Rafailidis², Maria Kalogirou³, Dimitrios Patoulas^{4,*}

ABSTRACT

The incidence of a second branchial arch sinus accounts for 26–60% of all existing congenital malformations deriving from the branchial apparatus. They are most usually detected between 14 months and 7 years of age, while their incidence during neonatal period and infancy accounts for 0.06% of all cases.

The aim of this case study is to emphasize three rare characteristic features: the manifestation during neonatal period, the bilateral localization and the ultrasonographic diagnostic documentation.

A 25 days old girl was admitted by her parents due to the presence of mucoid excretion from two small openings found on the neck. These openings were found bilaterally, between the mid and lower third of the anterior border of sternocleidomastoid muscle. Diagnosis was confirmed via ultrasonography. The patient underwent elective surgery during early infancy and both branchial fistulas were excised. Patient's postoperative course was uneventful.

In conclusion:

- in cases of a bilateral second branchial arch sinus, the branchio-oto-renal (BOR) or branchio-otic (BO) syndromes must be excluded;
- ultrasound scan can be used for the thorough evaluation of the sinus anatomic course and the relationship with the adjacent anatomic structures;
- prompt diagnosis and early therapeutic intervention, even during neonatal period, ensures an uneventful post-operation course.

KEYWORDS

bilateral branchial sinus; second branchial arch; ultrasonography; neonate

AUTHOR AFFILIATIONS

¹ 1st Department of Pediatric Surgery, Aristotle University of Thessaloniki, General Hospital 'G. Gennimatas', Thessaloniki, Greece

² Department of Radiology, Aristotle University of Thessaloniki, General Hospital 'AHEPA', Thessaloniki, Greece

³ National Health Center of Kalambaka, Trikala, Greece

⁴ Department of Internal Medicine, General Hospital of Veria, Veria, Greece

* Corresponding author: M. Alexandrou 3B, Peuka, Thessaloniki, Postal code 57010; e-mail: dipatoulas@gmail.com

Received: 29 January 2018

Accepted: 2 March 2018

Published online: 2 July 2018

Acta Medica (Hradec Králové) 2018; 61(1): 33–36

<https://doi.org/10.14712/18059694.2018.21>

© 2018 The Authors. This is an open-access article distributed under the terms of the Creative Commons Attribution License (<http://creativecommons.org/licenses/by/4.0>), which permits unrestricted use, distribution, and reproduction in any medium, provided the original author and source are credited.

INTRODUCTION

“Branchia” is the Greek word for gill, and the same word describes the corresponding anatomic structures, due to their resemblance to fish gills. Branchial apparatus plays a vital role in the development of head and neck structures. Six paired branchial arches, develop from the 4th to the 6th fetal week. Each branchial arch consists of a mesenchymatous core covered externally by ectoderm and internally by endoderm (1).

The incidence of second branchial arch deformities accounts for 26–60% of all existing congenital malformations deriving from the branchial apparatus. They are most frequently detected between the 14th month and the 7th year of life, while their incidence during neonatal period and infancy accounts for 0.06% of all cases (2) Second branchial sinuses are the most common branchial anomalies (up to 97% of all second branchial apparatus anomalies) and they are usually found unilaterally (2, 3).

The aim of this case study is to emphasize four uncommon features: the manifestation during neonatal period, the bilateral localization, the ultrasonographic diagnostic documentation and the absence of branchio-oto-renal (BOR) syndrome features.

CASE REPORT

A 25 days old girl was admitted to our Department by her parents due to the presence of mucoïd excretion from two small openings found on the neck. These openings were found bilaterally, between the mid and lower third of the anterior border of sternocleidomastoid muscle (Figures 1, 2).

Ultrasonography revealed the presence and anatomic course of two branchial sinuses, 1.2–1.3 mm in diameter. They were located subcutaneously, penetrating the platysma, passing between the carotid bifurcations and leading to the peritonsillar fossa (Figure 3).

Preoperative evaluation did not reveal any abnormality, while familial predisposition was not documented. More specifically, in the context of thorough physical examination there were no distinctive features indicative of cranio-facial deformities or ocular abnormalities. ENT examination was also normal, without indications of hearing loss. Ultrasonographic evaluation of the urinary tract did not reveal any pathology.

The patient then underwent elective surgery under general anaesthesia. The two branchial sinus tracts were initially catheterized with the use of a 4 Fr catheter. These were then used to lead in, while the sinus tract was dis-



Fig. 1, 2 External opening of the right (figure 1 – arrow) and left sinus (figure 2 – arrow), respectively.

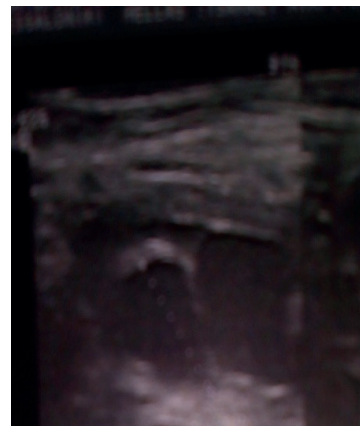


Fig. 3 Ultrasonographic image of the right branchial sinus.

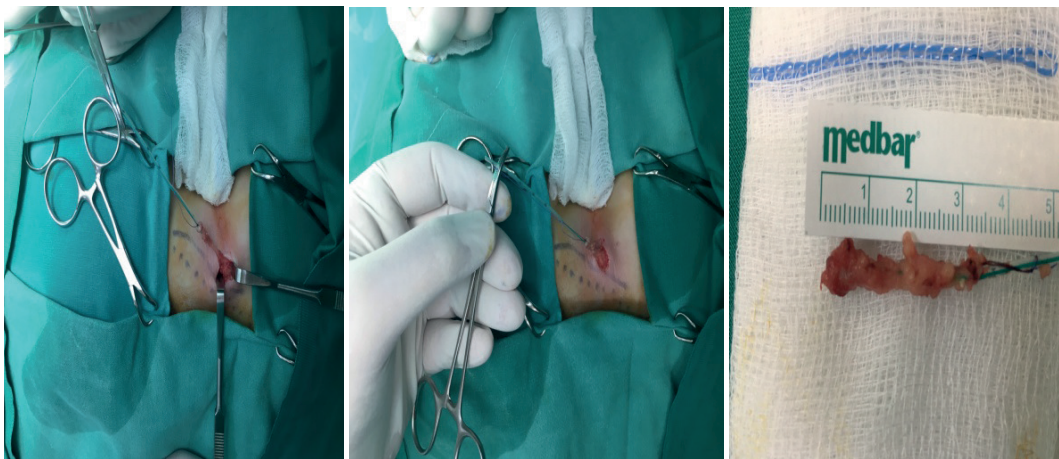


Fig. 4–6 Notice the step by step meticulous dissection of the left branchial sinus.

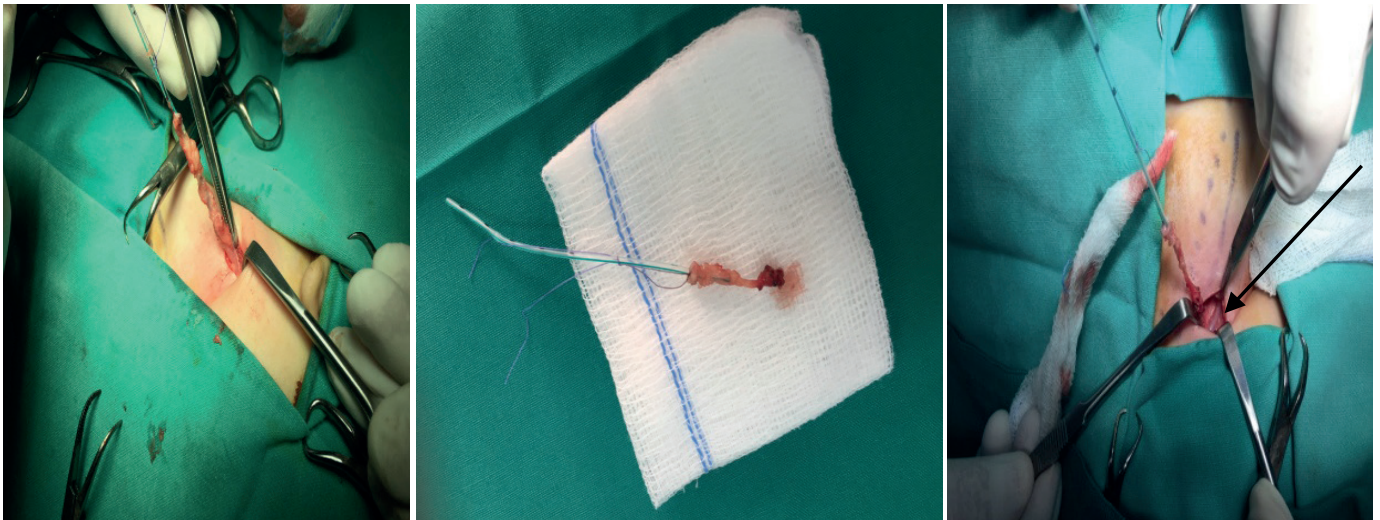


Fig. 7-9 Notice the step by step meticulous dissection of the right branchial sinus, passing between the carotid bifurcation. Figure 8 depicts the internal jugular vein and under this, the internal carotid artery (arrow)

sected through a step-ladder incision until the complete excision of each tract at the level of tonsillar fossa. A second incision was not required. Traction of the leading catheter assisted to the better dissection of the branchial sinus (Figures 4-9).

Patient's postoperative course was uneventful and she was discharged home the next day in good general condition. The excised specimens were subjected to histopathological examination, which showed that they were lined by squamous epithelium, while cartilage remnants and lymphoid tissue were found in the subepithelium.

One year later, patient remains asymptomatic without indications of recurrence.

DISCUSSION

Anomalies of the second branchial arch can be found in the anterior-lateral surface of the neck along with the anterior border of the sternocleidomastoid muscle. Classification of second branchial apparatus sinuses is based upon their anatomic course and the relationship with the adjacent anatomic structures (Table 1). In this case report, we present a type III second branchial sinus (3).

After meticulous research of the relevant literature, there are less than 7 reports of second branchial sinuses found bilaterally, while 6 of them were associated with familial predisposition (4-8). Bilateral manifestation along with absence of familial predisposition were the two key points in our case.

Clinical manifestation of a second branchial fistula during neonatal period is very rare, even when it manifests unilaterally. After meticulous bibliographic research, we did not find another case of second branchial fistula diagnosed during neonatal period (9-13). Prasad and colleagues reported another case of remnant of the second branchial apparatus, which was diagnosed and surgically treated at the age of 5 months, without determination of the specific type of this anomaly (3).

Tab. 1 Classification of second branchial apparatus sinuses.

Type	Characteristics
I	Branchial sinus penetrates the platysma and ends to the deep cervical fascia
II	Branchial sinus extends medially between the external and internal carotid artery
III	Branchial fistula passes between carotid bifurcation, then penetrates the stylohyoid muscle and the posterior surface of the digastric muscle towards ipsilateral pharynx to end up to the tonsillar fossa. Rarely, there are two complete openings. The sinus passes next to the glossopharyngeal and hypoglossal nerves, behind the stylohyoid ligament.
IV	Branchial sinus passes between the carotid artery bifurcation and ends blindly.

In the largest relevant retrospective study, Yang and colleagues report 28 cases of branchial apparatus anomalies that they encountered, while, only 5 of them (16.7%) derived from the second branchial apparatus. The youngest patient of their study group was 1 year old (14). Smith and Kielnovitch reported a case of a newborn with branchial cyst, remnant of second branchial apparatus (15).

In a retrospective study conducted by Maddalozzo and colleagues, including 28 cases in total, three patients (11%) had bilateral second branchial arch sinus. In two out of those three cases (66%) there were features indicative of BOR syndrome. Mutation of EYA1 gene is implicated as the commonest cause of BOR syndrome. In cases of this syndrome, hearing loss's incidence reaches up to 90%, with the mixed type being the most prevalent. Hearing loss may progress during the course of life in 12.8% of all cases (12). There are also cases, in which no renal involvement is documented, thus it is called branchial-otic (BO) syndrome (16).

In terms of exclusion of BOR syndrome in our case, we used the criteria proposed by Chang and colleagues. Based upon those criteria, in order to establish the diagnosis, the patient must fulfill three major criteria or two major and

two minor criteria, when there is no familial predisposition. Our patient fulfilled only one major criterion, the presence of bilateral second branchial arch anomalies, with no minor criteria. Thus, the clinical diagnosis of BOR syndrome was excluded. After that, we did not consider as necessary the performance of genetic testing in our patient (17).

Determination of the anatomic course of a second branchial sinus constitutes the basis for safe and successful treatment. Most frequently used methods for this aim are: a) conduction of fistulogram preoperatively and b) intraoperative injection of blue de methylene via the external opening of the sinus (1-3).

However, Prasad et al., in their series consisting of 17 cases of second branchial sinus, documented the anatomic course via ultrasonography in 9 patients (3). In our case, ultrasonography contributed crucially to the preoperative determination of the anatomic course of the sinuses.

There is indication of surgical excision of second branchial sinus early after diagnostic documentation. Major risks are: suppuration development of solid adhesions that lead to laborious and unsafe surgical excision, due to the adjacency to major vessels and hypoglossal nerve. Another main risk that must be avoided in clinical practice is the possible development of branchial carcinoma in the future (3). Alternative treatment methods such as endoscopic electro-coagulation and chemical cauterization are considered as unsafe in pediatric population (18).

In conclusion:

- in cases of a bilateral second branchial arch sinus, the branchio-oto-renal (BOR) or branchio-otic (BO) syndromes must be excluded;
- ultrasound scan can be used for the thorough evaluation of the sinus anatomic course and the relationship with the adjacent anatomic structures;
- prompt diagnosis and early therapeutic intervention, even during neonatal period, ensures an uneventful post-operation course.

REFERENCES

1. Waldhausen JH. Branchial cleft and arch anomalies in children. *Semin Pediatr Surg* 2006; 15(2): 64-9.
2. Singh AP, Kumar V, Narula V, Meher R, Raj A. Bilateral first and second arch anomalies: a rare presentation. *Singapore Med J* 2012; 53(4): e74-6.
3. Prasad SC, Azeez A, Thada ND, Rao P, Bacciu A, Prasad KC. Branchial anomalies: diagnosis and management. *Int J Otolaryngol* 2014; 2014: 237015.
4. Gupta AK, Kumar S, Jain A. Bilateral first and second branchial cleft fistulas: a case report. *Ear Nose Throat J* 2008; 87: 291-3.
5. Schewitsch I, Stalsberg H, Schroder KE, Mair IW. Cysts and sinuses of the lateral head and neck. *J Otolaryngol* 1980; 9: 1-6.
6. Gatti WM, Zimm J. Bilateral branchial cleft fistulas: diagnosis and management of two cases. *Ear Nose Throat J* 1988; 67: 256, 258, 261.
7. Shvero J, Hadar T, Avidor I, Abraham A, Sidi J. Heterotopic salivary tissue and branchial sinuses. *J Laryngol Otol* 1986; 100: 243-6.
8. Rohini M, Yogesh S, Neha S, Rima D. Bilateral complete second branchial cleft fistula: case report and its embryological review. *Indian Med Specialities* 2013; 4(2): 305-7.
9. Schroeder JW Jr, Mohyuddin N, Maddalozzo J. Branchial anomalies in the pediatric population. *Otolaryngol Head Neck Surg* 2007; 137(2): 289-95.
10. Kajosaari L, Mäkitie A, Salminen P, Klockars T. Second branchial cleft fistulae: Patient characteristics and surgical outcome. *Int J Pediatr Otorhinolaryngol* 2014; 78(9): 1503-7.
11. Cheng J, Elden L. Management of pediatric second branchial fistulae: Is tonsillectomy necessary? *Int J Pediatr Otorhinolaryngol* 2012; 76(11): 1601-3.
12. Maddalozzo J, Rastatter JC, Dreyfuss HF, Jaffar R, Bhushan B. The second branchial cleft fistula. *Int J Pediatr Otorhinolaryngol* 2012; 76(7): 1042-5.
13. Bajaj Y, Ifeacho S, Tweedie D et al. Branchial anomalies in children. *Int J Pediatr Otorhinolaryngol* 2011; 75(8): 1020-3.
14. Teo NW, Ibrahim SI, Tan KK. Distribution of branchial anomalies in a paediatric Asian population. *Singapore Med J* 2015; 56(4): 203-7.
15. Smith JF, Kielnovitch I. Branchial cyst anomaly in a newborn. *Otolaryngol Head Neck Surg* 1989; 100(2): 163-5.
16. Trummer T, Müller D, Schulze A, Vogel W, Just W. Branchio-oculo-facial syndrome and branchio-otic/branchio-oto-renal syndromes are distinct entities. *J Med Genet* 2002; 39(1): 71-3.
17. Chang EH, Menezes M, Meyer NC, et al. Branchio-oto-renal syndrome: the mutation spectrum in EYA1 and its phenotypic consequences. *Hum Mutat* 2004; 23(6): 582-9.
18. Thakur JS, Shekar V, Saluja M, Mohindroo NK. Coexistence of bilateral first and second branchial arch anomalies. *BMJ Case Rep* 2013; 2013 pii: bcr2013008698.

Fountain's Sign as a Diagnostic Key in Acute Idiopathic Scrotal Edema: Case Report and Review of the Literature

Dimitrios Patoulas^{1,*}, Vasileios Rafailidis², Thomas Feidantsis³, Maria Kalogirou⁴, Dimitrios Rafailidis⁵, Ioannis Patoulas³

ABSTRACT

The acute idiopathic scrotal edema (AISE) is a self-limited disease of unknown etiology, characterized by edema and erythema of the scrotum and the dartos, without expansion to the underlying layers of scrotum's wall or to the endoscrotal structures. Boys younger than 10 years old are usually involved in 60–90% of all cases. Diagnosis is made after exclusion of other causes of acute scrotum.

We present a case of a 7-year old boy, who was admitted to the Emergency Department due to development of scrotal edema and erythema over the last 48 hours, which extended to the base of the penis. The patient mentioned that he first noticed the erythema on the anterior surface of the right hemiscrotum, which gradually extended. Physical examination did not reveal presence of pathology involving the endoscrotal structures, indicative of need for urgent surgical intervention. Transillumination was negative for blue dot sign. Ultrasonographic examination of the scrotum documented the homogeneity of the testicular parenchyma, while color Doppler revealed the presence of fountain's sign (equal arterial blood supply to both testicles). Conservative strategy was followed and the patient gradually improved within the next three days.

In conclusion, meticulous physical examination along with ultrasonographic examination of the suffering scrotum, especially with the highlighting of fountain's sign with color Doppler, document the diagnosis of AISE. Thus, need for urgent surgical investigation of the suffering scrotum due to diagnostic doubt is limited.

KEYWORDS

acute idiopathic scrotal edema; Fountain's sign; color Doppler; endoscrotal structures

AUTHOR AFFILIATIONS

¹ Department of Internal Medicine, General Hospital of Veria, Veria, Greece

² Department of Radiology, Aristotle University of Thessaloniki, General Hospital 'AHEPA', Thessaloniki, Greece

³ 1st Department of Pediatric Surgery, Aristotle University of Thessaloniki, General Hospital 'G. Gennimatas', Thessaloniki, Greece

⁴ Health Center of Kalambaka, General Hospital of Trikala, Trikala, Greece

⁵ Department of Radiology, General Hospital 'G. Gennimatas', Thessaloniki, Greece

* Corresponding author: M. Alexandrou 3B, Pefka, Thessaloniki, Postal code 57010; e-mail: dipatoulas@gmail.com

Received: 5 November 2017

Accepted: 27 March 2018

Published online: 2 July 2018

Acta Medica (Hradec Králové) 2018; 61(1): 37–39

<https://doi.org/10.14712/18059694.2018.22>

© 2018 The Authors. This is an open-access article distributed under the terms of the Creative Commons Attribution License (<http://creativecommons.org/licenses/by/4.0>), which permits unrestricted use, distribution, and reproduction in any medium, provided the original author and source are credited.

INTRODUCTION

Of all the clinical entities that come under the term “acute painful scrotum” in childhood, 2.3% of those cases are attributed to AISE (1, 2). The age distribution of clinical manifestation of acute scrotal edema ranges from 5 to 11 years. In 60–90% of all cases, AISE manifests in boys 10 years old or less (1).

It is a self-limited disease of unknown etiology, characterized by edema and erythema of the scrotum and the dartos, without expansion to the underlying layers of scrotum’s wall or to the endoscrotal structures. Typically, it starts from the groin or the perineum with rapid expansion to the scrotum (2).

Aim of the present case study is to make a suggestion regarding the need for substantial modification of diagnostic approach in potential cases of AISE. In other words, diagnostic documentation should not be made on the basis of exclusion, but with the highlighting the crucial role of fountain’s sign as a diagnostic key.

CASE DESCRIPTION

A 7-year old boy was admitted to the Emergency Department, due to development of scrotal edema and erythema over the last 48 hours, which extended to the base of the penis. The patient noticed that the erythema started from the anterior surface of the right hemiscrotum and gradually extended to the whole anterior surface of the scrotum and to the penile basis (Figure 1).

Meticulous physical examination did not reveal findings indicative of pathology of endoscrotal structures. Both testicles were of equal size, painless and orthotopic, with vertical orientation and normal turgidity. The patient complained for pain during the palpation of the right testicle, however, this was not a stable finding. Cremasteric muscle reflex was produced bilaterally. Palpation of epididymis was painless bilaterally, without observation



Fig. 1 Notice the erythema and the edema on the anterior surface of the right hemiscrotum, which gradually involved the anterior surface of the entire scrotum.



Fig. 2 Fountain’s sign, as depicted in color Doppler examination in our case.

of edema, while Prehn’s sign was negative. Blue dot sign also turned out negative during transillumination.

Ultrasonographic examination of the suffering scrotum followed and revealed the homogeneity of the testicular parenchyma, while we also measured the thickness of the scrotal wall, which was 7.2 mm. Color Doppler documented the equal arterial blood supply to both testicles, finding consistent with fountain’s sign (Figure 2).

As there was no clinical or imaging indication of surgical investigation of the suffering scrotum, we decided to treat our patient conservatively. He actually improved within the next three days after admission. He was discharged home after the 3rd day of hospitalization in good general condition. The patient was re-examined as an outpatient 10 and 20 days after admission, without evidence, both clinical and ultrasonographic, of pathology involving the endoscrotal structures.

DISCUSSION

The etiology of AISE is currently unknown, although certain situations have occasionally been implicated in the pathogenesis of this entity, such as:

1. The cellulitis, that extends from the perianal region to the scrotum. This approach lacks, because, on the one hand, the cultures received from the region are usually negative, and on the other hand, the AISE is mainly self-limited without therapeutic intervention.
2. The bites caused by insects.
3. An injury.
4. The urine loss, which causes aseptic inflammatory response in the area, expanding to the scrotum.
5. The allergy. It is considered as the most likely cause; based on the fact that eosinophilia is found in more than 40% of all AISE cases, while these patients also suffer from diseases such as asthma, eczema or contact

dermatitis. Besides, there is evidence that medication with antihistamines contributes to the recession of the symptoms. Thus, it is believed that AISE is a clinical manifestation of angioedema (3, 4).

6. The acute Epstein-Barr viral (EBV) infection (5).

These patients usually do not complain of accompanying symptoms. They can rarely mention indistinct discomfort in the suffering scrotum. Rarely, itchiness precedes edema. Generally, scrotal edema is the first clinical manifestation; it develops suddenly and is accompanied with diffuse erythema in the affected area. AISE spreads rapidly, within a few hours. Edema most often begins unilaterally (L/R = 1), but it progressively extends to the whole scrotum. Erythema expands to the groin (67% of all cases), the perineum (42%), the penis (20%) or to the suprapubic region. Edema and erythema are the major clinical manifestations of AISE, while local pain coexists in 80% of all cases. The duration of the above mentioned clinical manifestations usually ranges from 6 to 72 hours (average 14 hours) (1, 2). Soon begins the recession of edema and erythema, which is usually complete within 48 hours, without residual signs. In 21% of all cases, AISE recurs from 1 to 3 times, without complication. Relapse occurs several months or even years after the prior event.

Regarding differential diagnosis based upon physical examination, pathognomonic clinical signs in cases of testicular torsion are the absence of cremasteric muscle reflex and the high position of the testicle. In cases of appendiceal torsion, localized tenderness and pain during palpation of the upper pole of the suffering testicle and positive blue dot sign in transillumination of the suffering hemiscrotum are pathognomonic (1, 2, 6). Finally, in acute epididymitis, pain during palpation of the suffering epididymis, along with the presence of edema, are typical.

Major imaging modality is color Doppler, as it contributes substantially to the exclusion or confirmation of other main causes of acute scrotum – most significantly, of those requiring urgent surgical intervention, soon after diagnosis –, and to the diagnostic documentation of AISE, with the highlighting of pathognomonic findings, including fountain's sign (7–10).

Exclusion of the testicular torsion can be made accurately, after conduction of high resolution ultrasound imaging with the use of frequencies 10–12 MHz: basic indication of testicular torsion is the observation of rotations of the spermatic cord (snail-shell shaped mass), and not the disruption of the testicular circulation (11). High resolution ultrasound features 96% sensitivity, while color Doppler ultrasound is inferior, with 76% sensitivity (11, 12).

After performing cross sections, the homogenous thickening of the scrotal wall is documented, ranging from 3.4 to 13.4 mm (average 7.7–11.2 mm), as in our case. A second pathognomonic finding is the increased vascularization of the scrotal wall, which is not always helpful in pediatric population (10, 13).

Blood supply to the scrotum is ensured by the anterior and posterior scrotal artery, which originate from deep branches of the internal and external pudendal artery. Depiction of those vascular branches in cross sections, along with observation of the scrotal hyperemia, constitutes the characteristic fountain's sign (7, 8, 14, 16). Other potential

ultrasonographic findings are the development of reactive hydrocele, which occurs in 20% of all AISE cases, and the presence of swollen and hyperemic inguinal lymph nodes (1). None of the aforementioned findings was observed in our case.

CONCLUSION

Formerly, diagnosis of AISE was made via the exclusion of other causes of acute painful scrotum. Meticulous physical examination by the pediatric surgeon with precise interpretation of the clinical findings, along with the depiction of pathognomonic signs in color Doppler, and especially of fountain's sign, are crucial for the correct diagnosis. Thus, the necessity of urgent surgical investigation of the suffering scrotum due to diagnostic doubt – especially for the documentation or exclusion of testicular torsion – is significantly restricted.

CONFLICT OF INTEREST

None of the contributing authors have any conflict of interest, including specific financial interests or relationships and affiliations relevant to the subject matter or materials discussed in the manuscript.

REFERENCES

1. Klin B, Lotan G, Efrati Y, Zlotkevich L, Strauss S. Acute idiopathic scrotal edema in children – revisited. *J Pediatr Surg* 2002; 37(8): 1200–2.
2. Holcomb GW, Murphy JP, Ostlie DJ. In: Ashcraft's Pediatric Surgery Sixth Ed., Chapter: Acute Scrotum. Saunders Elsevier 2014, p. 705.
3. Van Langen AM, Gal S, Hulsmann AR, De Nef JJ. Acute idiopathic scrotal oedema: four cases and a short review. *Eur J Pediatr* 2001; 160(7): 455–6.
4. Weinberger LN, Zirwas MJ, English JC III. A diagnostic algorithm for male genital oedema. *J Eur Acad Dermatol Venereol* 2007; 21(2): 156–62.
5. Lee SH. Acute idiopathic scrotal edema caused by Epstein-Barr Virus. *Pediatr Infect Dis J* 2016; 35(5): 593.
6. Molokwu CN, Somani BK, Goodman CM. Outcomes of scrotal exploration for acute scrotal pain suspicious of testicular torsion: a consecutive case series of 173 patients. *BJU Int* 2011; 107(6): 990–3.
7. Breen M, Murphy K, Chow J, Kiely E, O'Regan K. Acute idiopathic scrotal edema (case report). *Case Rep Urol* 2013; 2013: 829345.
8. Geiger J, Epelman M, Darge K. The fountain sign: a novel color Doppler sonographic finding for the diagnosis of acute idiopathic scrotal edema. *J Ultrasound Med* 2010; 29(8): 1233–7.
9. Copertino M, Benelli E, Gregori M, Barbi E, Ventura A. A shining scrotal fountain. *J Pediatr* 2015; 167(1): 205.e1.
10. Mesquita RD, Rosas JL. Adult acute scrotal edema-when radiologists can help to avoid unnecessary surgical treatment. *J Radiol Case Rep* 2017; 11(8): 24–30.
11. Aso C, Enriquez G, Fité M, et al. Gray-scale and color Doppler sonography of scrotal disorders in children: an update. *Radiographics* 2005; 25(5): 1197–214.
12. Carkaci S, Ozkan E, Lane D, Yang WT. Scrotal sonography revisited. *J Clin Ultrasound* 2010; 38(1): 21–37.
13. Lee A, Park SJ, Lee HK, Hong HS, Lee BH, Kim DH. Acute idiopathic scrotal edema: Ultrasonographic findings at an emergency unit. *Eur Radiol* 2009; 19(8): 2075–80.
14. Yusuf GT, Sidhu PS. A review of ultrasound imaging in scrotal emergencies. *J Ultrasound* 2013; 16(4): 171–8.
15. Roic G. Sonography of the acute scrotum in children. *Pediatrics Today* 2016; 12(1): 65–74.
16. Tietze A, Avula S. Acute Idiopathic Scrotal edema. *Euro Rad* 2008; Case 6477.

Reviewer, Thank You

The editors greatly appreciate the support of all reviewers whose comments and scientific evaluation of submitted manuscripts are invaluable for ensuring the scientific quality of this journal. The following distinguished clinicians and scientists acted as reviewers:

Zdeněk Adam, *Brno, Czech Republic*
 Boon Huat Bay, *Singapore*
 Vladimíra Bednářová, *Prague, Czech Republic*
 Petra Bělohávková, *Hradec Králové, Czech Republic*
 Helmut Beltraminelli, *Bern, Switzerland*
 Jan Betka, *Prague, Czech Republic*
 Andras Bikov, *Budapest, Hungary*
 Paolo Boffano, *Aosta, Italy*
 Piotr Brzezinski, *Ustka, Poland*
 Jan Bureš, *Hradec Králové, Czech Republic*
 Jan Čáp, *Hradec Králové, Czech Republic*
 Zuzana Červinková, *Hradec Králové, Czech Republic*
 Viktor Chrobok, *Hradec Králové, Czech Republic*
 Jiří Cyrany, *Hradec Králové, Czech Republic*
 Marina Goncalves Diniz, *Belo Horizonte, Brazil*
 Petr Dítě, *Ostrava, Czech Republic*
 Tatjana Dostálová, *Prague, Czech Republic*
 Nicole Doudican, *New York, USA*
 Pavel Drastich, *Prague, Czech Republic*
 Ivo Dřížhal, *Hradec Králové, Czech Republic*
 Josef Dvořák, *Prague, Czech Republic*
 Edvard Ehler, *Pardubice, Czech Republic*
 Karel Ettler, *Hradec Králové, Czech Republic*
 Attila Feher, *New Haven, Connecticut, USA*
 Igor Guňka, *Hradec Králové, Czech Republic*
 Abdubaset Hafuda, *Pardubice, Czech Republic*
 Eduard Havel, *Hradec Králové, Czech Republic*
 Emir Haxhija, *Graz, Austria*
 Zbyněk Hrnčíř, *Hradec Králové, Czech Republic*
 Petr Hůlek, *Hradec Králové, Czech Republic*
 William H James, *London, United Kingdom*
 Young-Sik Jung, *Daejeon, South Korea*
 Suleyman Kaplan, *Samsun, Turkey*
 Stamatis Katsenos, *Athens, Greece*
 Charanjit Kaur, *Singapore*
 Dmitry Kazakov, *Pilsen, Czech Republic*
 Jan Klener, *Prague, Czech Republic*
 Miloslav Kmonicek, *Bristol, United Kingdom*
 Vladimír Koblížek, *Hradec Králové, Czech Republic*
 Radim Kočvara, *Prague, Czech Republic*
 Jaroslav Koudelka, *Hradec Králové, Czech Republic*
 Ronald G. Lawler, *Providence, Rhode Island, USA*
 Alexander Lerchl, *Bremen, Germany*
 Jan Libiger, *Hradec Králové, Czech Republic*
 Mojmír Mach, *Bratislava, Slovak Republic*
 Jaroslav Malý, *Hradec Králové, Czech Republic*
 Wolfgang Maret, *London, United Kingdom*
 Bohuslav Melichar, *Olomouc, Czech Republic*
 Vlad Melnikov, *Novosibirsk, Russia*
 Adamantios Michalinos, *Athens, Greece*
 Bryan Moon, *Houston, Texas, USA*
 Jiří Náhlavský, *Hradec Králové, Czech Republic*
 Umavedi P. Nair, *Gainesville, Florida, USA*
 Dimitar Hadži Nikolov, *Kolín, Czech Republic*
 Ivo Novák, *Hradec Králové, Czech Republic*
 Jose Boix Ochoa, *Barcelona, Spain*
 Daniela Pelclová, *Prague, Czech Republic*
 Jiří Petera, *Hradec Králové, Czech Republic*
 Georg Petroianu, *Miami, Florida, USA*
 Unni Krishnan Pillai, *Brisbane, Australia*
 René Pita, *Madrid, Spain*
 Maurizio Quadri, *Asti, Italy*
 Robert S. Redman, *Washington, D.C., USA*
 Ivono Riva, *Rome, Italy*
 Kamil Rudolf, *Hradec Králové, Czech Republic*
 Hiroaki Satoh, *Mito, Ibaraki, Japan*
 Petr Sedláček, *Prague, Czech Republic*
 Radovan Slezák, *Hradec Králové, Czech Republic*
 Alena Šmahelová, *Hradec Králové, Czech Republic*
 Jiří Špaček, *Hradec Králové, Czech Republic*
 Radek Štichauer, *Hradec Králové, Czech Republic*
 Zdeněk Šubrt, *Hradec Králové, Czech Republic*
 Jakub Suchánek, *Hradec Králové, Czech Republic*
 Robert Tomáš, *Prague, Czech Republic*
 Václav Vacek, *Pilsen, Czech Republic*
 Jiří Vlček, *Hradec Králové, Czech Republic*
 Jan Vodička, *Pardubice, Czech Republic*
 Tom Wilson, *Leeds, United Kingdom*

The Editors hereby express their sincere gratitude for and their appreciation of the work done as well as the support given to this journal.